Review Paper

New frontiers in the biosynthesis of metal oxide nanoparticles and their environmental applications: an overview

Shushay Hagos Gebre[1] · **Marshet Getaye Sendeku**[2]

© Springer Nature Switzerland AG 2019

Abstract
Nanotechnology has become a promising and emerging field of research in creating and modifying nanomaterials for different applications. Nanoparticles are considered to be the basic element of nanotechnology as they are the primary source of several nanostructured materials. During the last few decades, several metal oxide nanoparticles (NPs) were synthesized and their applications were investigated in various fields of science and technology, including biomedical, environmental, energy and agricultural practices. Moreover, metal oxide NPs have been synthesized by physical and chemical methods, while the chemical method used different chemicals as reducing and stabilizing agents. However, the wet chemical synthesis strategy become responsible for various biological and environmental risks due to the toxicity of used chemicals. Recently, biological synthesis of metal oxide nanoparticles using plants, algae, and microbes as a source of precursor material has emerged as a green and safe method. Additionally, the green synthesized metal oxide nanoparticles have shown a pivotal role in several applications such as nano-adsorbents, nano-membranes, photocatalysts and disinfection of wastewater from microbes. In this review, we present an overview of the biosynthesis of metal oxide nanoparticles such as; ZnO, CeO_2, TiO_2, CdO, CuO, Fe_3O_4, SnO_2, NiO etc. Their method of characterization and properties is also discussed. Finally, their applications towards environmental protection is presented with particular attention to water treatment and remediation.

Keywords Metal oxide nanoparticle · Green synthesis · Photocatalytic · Nanomaterials · Environmental application

1 Introduction

Nanotechnology is an interdisciplinary area of research involving synthesis, characterization and applications of nanomaterials. It is one of the rapidly growing fields with significant applications in various areas for the past one decade [1, 2]. Nanomaterials (NMs) are nano-objects having a size range of 1–100 nm, at least in one dimension which have specific properties in terms of size, shape, porosity etc. [3–5]. The main reasons why nanomaterials have attracted great attention is due to their unique optical, electrical, magnetic, chemical and mechanical properties which is different from their bulk counterparts. The synthesized powdered products have a large surface area to volume ratio, which is their most important feature responsible for the widespread use in mechanics, optics, electronics, biotechnology, microbiology, environmental remediation, medicine, numerous engineering fields and material science [5–7].

Metal oxide nanoparticles have a size within a nanoscale range, which include both deliberately synthesized and naturally occurring particles resulting from natural and anthropogenic processes [8]. Transition metal oxide nanoparticles are an important class of materials due to their attractive magnetic, electronic and optical properties. This makes them preferable to be used in a variety of

✉ Shushay Hagos Gebre, shushayhagos@gmail.com; Marshet Getaye Sendeku, getaamar@gmail.com | [1]Department of Chemistry, College of Natural and Computational Science, Jigjiga University, P.O. Box 1020, Jigjiga, Ethiopia. [2]National Center for Nanoscience and Technology (NCNST), University of Chinese Academy of Sciences (UCAS), Beijing, China.

SN Applied Sciences (2019) 1:928 | https://doi.org/10.1007/s42452-019-0931-4

Received: 19 March 2019 / Accepted: 16 July 2019 / Published online: 27 July 2019

applications, such as; catalysis, sensors, lithium-ion batteries, and environmental applications etc. When compared with other classes of materials, transition metal oxides have variety of interesting properties which deserves to be studied in different applications [9, 10].

Physical and chemical methods are being used extensively for the production of metal oxide nanoparticles. However, these techniques require the use of very reactive and toxic reducing agents such as sodium borohydride and hydrazine hydrate, which cause undesired detrimental impacts on the environment, plant and animal life. Moreover, the use of sophisticated equipment, tedious procedures and rigorous experimental conditions are also remained as a big challenges [7, 11]. Thus, physical methods produce heterogeneous NPs with high consumption of energy, and chemical methods utilize synthetic capping, reducing and stabilizing agents, and eliminate non-ecofriendly byproducts though desired homogenous metallic NPs are obtained [12].

In addition the obtained nanoparticles cannot be used for medicinal purpose due to their health related effects [13]. Therefore, researchers have devoted considerable efforts to develop facile, effective and reliable green chemistry methods for the production of nanomaterials. Several biological sources such as such as; plant extracts, bacteria, actinomycetes, fungi, yeast, viruses, macro algae [14] waste aquacultural and horticultural food materials are already introduced as a precursors to produce stable and well-functionalized nanomaterial, where these precursors act as reducing and capping agents [7, 15, 16].

The progress of nanotechnology in the field of environmental engineering, especially in wastewater treatment, has opened new directions by applying new materials and devices [17]. The use of nanotechnology for environmental remediation has received substantial financial support as well as attention from service providers and the scientific community [18]. The application of the nanomaterials increases rapidly due to the continuing advancement of the nanotechnology and their environmental fate of engineered NPs and their effects on the ecosystem and human health [19]. Thus, the uncontrolled discharge of the nanoparticles on the other hand is a serious threat to the sustainability of the environment in which plants are responsible to accommodate the nanomaterials for further transportation [20]. Ahmed et al. [21] studied the impact of CuO and TiO_2 nanoparticles on cell cycle progression and induction of oxidative stress in onion root, and ant it was found that, they reduced the mitotic index (MI) by 28% and 17%, respectively. Additionally, the adsorption of the NPs onto the onion root upon penetration inside tissues can generate reactive oxygen species (ROS), which eventually induced oxidative perturbation leading to imbalance in redox homeostasis, genotoxic, and mito-depressive effects. ZnONP and Zn^{+2} penetrates into the plant tissue (onion) and generates ROS, which induces oxidative imbalance leading to mito-depressive genotoxic effects [22]. Similarly, CuONP accommodate in potato roots and shoots (341.6 ± 14.3 and 146.9 ± 8.1 µg/g), respectively, which can lead to an increase in reactive oxygen species [23].

The use of metallic nanomaterials in diverse industrial products increases their exposure to the various components of the environment; air, water, oil and alternative renewable energies [24]. These days, the green synthesized nanomaterials have been tested for a wide variety of applications and showed many positive and promising activities. For example, ZnONPs prepared from *Hibiscus subdariffa, Azadirachta indica* and *Aloe vera* plant extracts were investigated for their potential use in bactericidal, antidiabetic and anti-fungal activities, and showed promising results [25, 26]. Additionally, nanosized ZnO synthesized using the same method from different plant sources has confirmed to be an efficient photocatalyst for degradation of organic pollutants [26–28].

Biogenically synthesized maghemite nanoparticles (γ-Fe_2O_3) using *Tridax* leaf extract exhibited 85% removal efficiency of Pb within 2 h and 96% in 24 h. Also, significant removal of Cd, reaching below the detection value (0.01 ppm in 2 h) was observed [29].

Works by Raghavendra et al. [30] show the potential use of green synthesized ZnONPs for biodiesel production. In typical synthesis experiment, water extracted *Garcinia gummi-gutta* seed (10 mL) was homogenized with $Zn(NO_3)_2{\cdot}6H_2O$ (2.32 g), dried and calcined in a muffle furnace at 450 °C. According to the authors, irregular shaped morphology with spongy cave-like structures having an average crystallite size of 14 nm was obtained. The biosynthesized ZnONPs was used for biodiesel production and *G. gummi-gutta* oil itself was also used as source of biodiesel. 1.5% w/v of ZnONPs were added to the CH_3OH (9:1) CH_3OH to oil molar ratio and the resultant mixture was added to the preheated oil. After the transesterification process, the yield of biodiesel obtained using ZnO nanocatalyst was found to be 80.1%. The use of nanocatalyst provides easy separation of products, higher catalytic activity, lesser pollution and reuse.

In recently study by Karthik et al. [31], ZnONPs were fabricated from *Acalypha indica* leaf extract and their potential was investigated for antimicrobial activities. Aqueous extract of the leaf was added to 0.5 g of 1 M zinc acetate under stirring for 1 h at 60 °C. The obtained precipitate was

then washed with deionized water several times and then heated in a hot-air oven at 80 °C for 24 h. The obtained ZnO nano-powders were calcined at three different temperatures, namely at 100, 300, and 600 °C. ZnONP600 shows spherical morphology, whereas ZnONP100 and ZnONP300 nanoparticles appear in irregular shape with an aggregated morphology. The average particle size of the ZnO nanoparticles observed through TEM images was 19.9, 53.39, and 65.13 nm for ZnONP100, ZnONP300, and ZnONP600, respectively. Thus, high temperature calcination of ZnO nanoparticles enhances their crystallinity due to particle growth and decreasing the defects in crystals. It is also found that the fabrics coated with ZnO nanocomposite obtained by calcination at 600 °C show maximum zone of inhibition against *E. coli* (25.13 ± 0.05 mm) and *S. aureus* (30.17 ± 0.03 mm), higher UV-protection (87.8 UPF), and water-repellent property with enhanced wash durability than those coated with particles calcined at 100 and 300 °C.

Biological synthesis strategy has recently gained several attentions because of the facile, environmentally benign and simple nature. Hence, this review mainly focuses on the recent advancements in the biosynthesis of metal oxide NPs. The approaches for the synthesis of different metal oxide nanomaterials using plant parts, bacteria, fungi, macro and microalgae are discussed in brief. Then, we summarize the application of those green synthesized metal oxides to tackle environmental problems. The mechanism of formation of metal oxide NPs using plant and microorganism sources is discussed in the context of different responsible metabolites. Finally, the review concludes with some future insight and prospects.

2 Synthesis of metal oxide nanoparticles

A wide range of physical, chemical and biological techniques have been developed to produce metal oxide nanoparticles of different sizes, shapes, and compositions as described in Fig. 1.

2.1 Physical method

This type of synthesis process basically depends upon the instrument types used in the experiment. Tube, furnace,

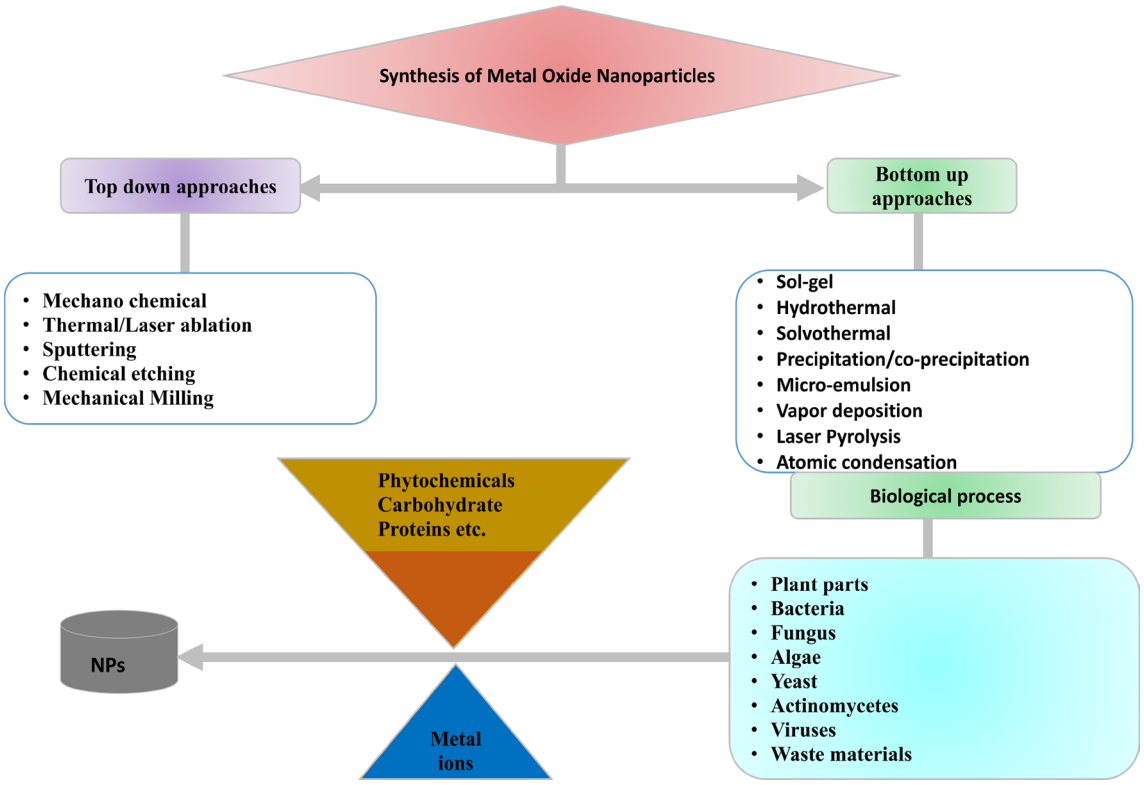

Fig. 1 Physico-chemical approaches and biological methods of nanoparticle synthesis

ceramic heater, laser ablation, ball milling, flame pyrolysis, and electric arc discharge are among the most commonly used methods for synthesis of the nanomaterials [32]. Ismail et al. [33] synthesized ZnO nanoparticle using laser ablation. The ablation in double distilled water yielded spherical nanoparticles in the average size of 35 nm. The use of water as a solvent has an important role in determining the size or shape of synthesized ablated particles. TiO_2 nanoparticle doped with Fe (10%) synthesized via ball-milling process in the average size of 25–30 nm for Rh-B degradation purpose. The doped nanoparticle shows highest photocatalytic efficiencies (higher than 60% at 120 min) under UV light irradiation [34].

2.2 Chemical method

Chemical method of synthesizing nanoparticles depends on chemicals, reducing agents and capping agents along with an optimum condition of temperature and pressure. They are relatively simple techniques, inexpensive, less instrumentation compared to many physical methods and can be carried even at lower temperature (< 350 °C) [32, 35]. Wet chemistry techniques using chemical approaches such as precipitation, sol–gel, and solvothermal processes are usually simpler and proved to be very effective for large-scale production [36]. Sol–gel synthesis of spherical shape zinc oxide nanoparticles using *Citrus aurantifolia* fruit extracts were produced by Samat and Nor [37] with a size range of 50–200 nm (FESEM) using zinc acetate as a metal ion source. The nanoparticles have a remarkable photocatalytic activity. Kulkarni [35] reported that solvothermal synthesized ZnO nanostructures show the average degradation of methylene blue 80% in 400 min. Moreover, Jagadhesan et al. [38] prepared Sb-doped ZnO nanoparticle via co-precipitation method. The Sb (0.075%) doped ZnO nanostructure improve the MB dye degradation efficiency (84%) compare to Sb (0.05%) doped ZnO nanostructures due to the creating of a large surface area.

2.3 Biological method

To reduce toxicity and improve efficacy of chemically synthesized NPs researchers have employed plant metabolites as adjuvant. The synthesis involves biological extract from microorganisms or plants as reducing agent to reduce metal ions either extracellularly or intracellularly. The extract components further act as capping agents and help in the production of homogenous and stable NPs through prevention of aggregation. This synthetic process is used for largescale production of NPs with biocompatibility, scalability, non-toxicity, reproducibility and medical applicability. Furthermore, metabolites that are used for reduction process are hypothesized to bind to the surface of NP and further enhance activity [12].

The choice of synthesis method determines the physicochemical characteristics of the metal oxide nanoparticle, such as the size, dispersity, type of intrinsic and/or extrinsic defects, morphology and crystal structure. As biocompatibility is one of the most important requirements for any nanomaterial used in the field of nanomedicine, biological method occurs as a good alternative, but the studies on biogenic synthesis methods are scanty and much work is necessary to improve their efficiency associated with size, shape and yield. Larger quantities of nanoparticles can be produced using chemical and physical methods and their main advantage over biological is the ability to control the size and shape [39].

Green synthesis of nanomaterials is a bottom-up approach (Fig. 1) similar to chemical reduction where an expensive chemical reducing agent is replaced by the extract of different biological sources plant parts, microorganisms, waste materials etc. Biological entities is easy (one-pot synthesis), fast, cost effective and eco-friendly process for the production of NPs [40]. There is an increasing need to develop high-yield, nontoxic, and environmentally benign procedures for the synthesis of metal oxide nanoparticles. A vast array of biological resources are available in nature including plants and plant products, algae, fungi, yeast, bacteria, and viruses could all be employed for the synthesis of metal oxides. Both unicellular and multicellular organisms have been known to produce intracellular or extracellular inorganic nanomaterials [15, 41]. The approach of using plant parts is more advantageous and straightforward in comparison with microorganisms since it does not need any special or complex procedures such as isolation, culture preparation, and culture maintenance. Furthermore, plant mediated synthesis of nanoparticles tends to be faster than microorganisms. Additionally, this phyto-mediated synthesis is cost-effective and relatively easy to scale up for the production of large quantities of nanoparticles [15].

2.3.1 Plant mediated biosynthesis of metal oxides nanoparticles

The use of plant system has been considered as a green route and a reliable method for the biosynthesis of metal oxide nanoparticles owing to its environmental friendly nature [42, 43]. In a biogenic synthesis of metal oxide nanoparticles, some phytochemicals such as alkaloids, terpenoids, polyphenols, tannin, phenolic acids and polysaccharides, present in the extracts of the plant stem, leaf

or flower, act as bio-reductant as well as capping agents [44–46]. The nature of the plant extract, concentration of the extract, the concentration of the metal salt, the pH, temperature and contact time are known to have a clear effect on the rate of production of the nanoparticles, their quantity and other characteristics (size, shape etc.) [47].

A facile, efficient and environmentally-friendly method has been developed by Rufus et al. [48] for the synthesis of hematite (α-Fe_2O_3) nanoparticles exploiting the reducing and capping potential of the aqueous leaf extract of the cashew tree (*Anacardium occidentale*). The Fe_2O_3 nanopartice synthesized in the size range 29–50 nm, as revealed by TEM and SEM micrographs. The as-synthesized Fe_2O_3 sample exhibited excellent antibacterial activity, which is demonstrated by inhibiting the growth of *E. coli* and *S. aureus*. The stability and bio-potency of the catalytically active hematite leads to functioned in the medical and environmental remediation.

Sundrarajan et al. [49] synthesized titanium dioxide (TiO_2) nanoparticles using leaf extract of *Morinda citrifolia* following advanced hydrothermal method. They characterized the synthesized nanomaterial using XRD, FTIR, SEM and EDX techniques. Interestingly, tetragonal rutile phase TiO_2 with an average crystallite size of 10 nm was obtained. The nanoparticles exhibited superior antimicrobial activity against microorganisms such as *S. aureus, E. coli, B. subtilis, P. aeruginosa, C. albicans, and A. niger*. The superior antimicrobial activity against gram-positive bacteria clearly demonstrated the antimicrobial value of synthesized TiO_2 nanoparticles against disease-causing pathogens. A noble synthesis of ZnO nanoparticle using *Annona squamosa* leaf extract as bio-reductant have shown fascinating antibiotic potentiation competence and anti-cancer activity with a targeted action through securing natural microbiome [50].

In recent work reported by Nasrollahzadeh and Sajadi [51] TiO_2NPs were synthesized from titanyl hydroxide using *Euphorbia heteradena Jaub* root extract as a reducing and capping agent. According to these authors, the hydroxyl groups of phenolics in *E. heteradena Jaub* root extract were not only responsible for the reduction of titanyl hydroxide but also function as capping ligands to the surfaces of TiO_2NPs (Fig. 2).

Green synthesis of multifunctional hexagonal wurtzite structured of zinc oxide nanoparticles with a variety of morphologies has been studied by Madan et al. [52]. They followed low-temperature solution combustion route, employing *Azadirachta indica* (Neem) leaf extract as template. The synthesized NPs were tested for their photocatalytic, photoluminescence, antioxidant and antibacterial activities. The antibacterial studies indicated that ZnONPs had significant antibacterial activity against *K. aerogenes* and *S. aureus* but not against *E. coli* and *P. aeruginosa*. Ali et al. [53] prepared ZnO nanoparticles following a cost-effective and efficient biogenic synthesis approach, exploiting the reducing and capping potential of *Aloe barbadensis Miller* (*Aloe vera*) leaf extract. The as-synthesized nanomaterial were used as antibiotics against multi-drug resistant clinical bacterial isolates. In another study, Sharma and his coworkers [54] used leaf extract of *Azadirachta indica* (Neem) plant as a reducing agent for

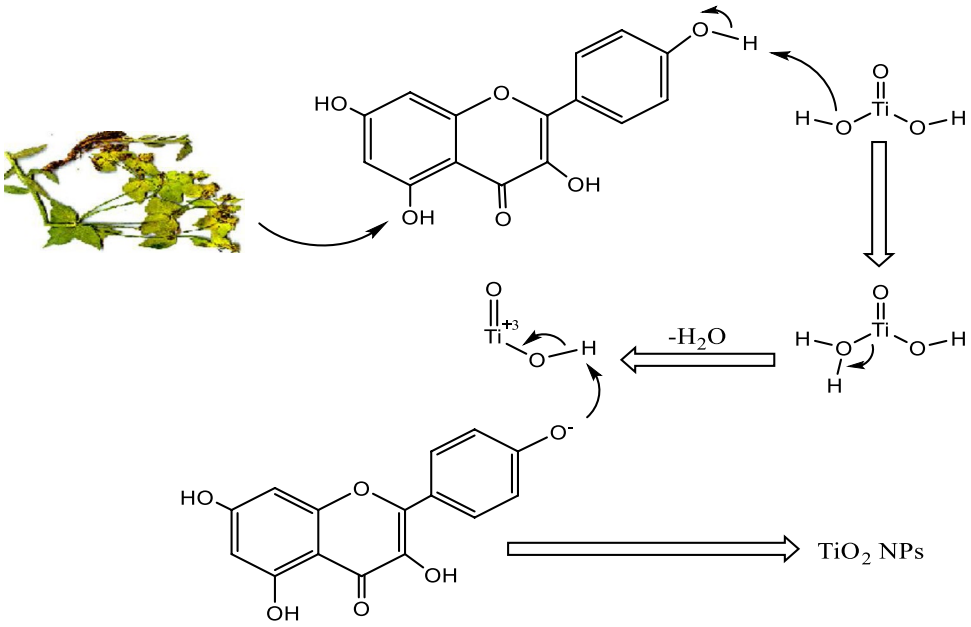

Fig. 2 Mechanism of bioreduction of titanyl hydroxide to TiO_2NPs using *Euphorbia heteradena Jaub* root extract as bio-template [51]. © Elsevier, reproduced with permission

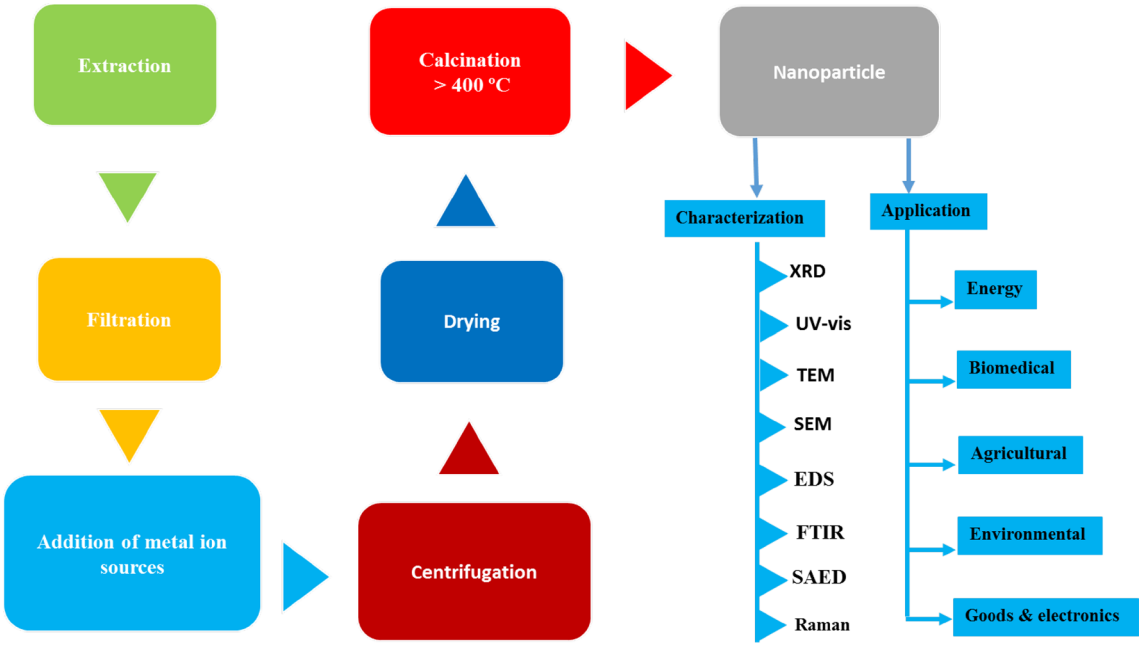

Fig. 3 Plant-mediated synthesis, characterization, and application of nanoparticle

the synthesis of nanosize tetragonal hausmannite crystals of Mn_3O_4. They applied the synthesized nanomaterial as a working electrode for fabricating an efficient chemical sensor for the detection of 2-butanone and also for the catalytic thermal decomposition of ammonium perchlorate by decreasing the decomposition temperature to 175 °C with a single decomposing step.

The presence of hazardous organic chemicals such as organic dyes in wastewater has been regarded as a major environmental concern, and it has drawn the attention of many researchers during the last few years. Over the last few decades, burgeoning researches were conducted and exciting results were obtained (Fig. 3). Basically, the pollutants are difficult to remove by natural processes due to their chemical and biological stabilities. A renewable and non-toxic leaf extract of *Euphorbia prolifera* was used by Momeni et al. [55] as a mild reducing agent as well as stabilizer. Through using this plant, 5–17 nm Cu/ZnO sized nanoparticles (NPs) were obtained. The synthesized composite nanomaterial exhibited excellent catalytic activity in degrading methylene blue and congo red dyes in their aqueous solutions in the presence of $NaBH_4$.

Green synthesis of iron (III) oxide nanorods mediated by polyphenols present in Omani mango *(Disambiguation)* tree leaves has been carried out by Al-ruqeishi et al. [56]. The synthesized Fe_2O_3 nanorods with an average length and diameter of 15 nm and 3 nm, respectively, were obtained. The as-synthesized material was

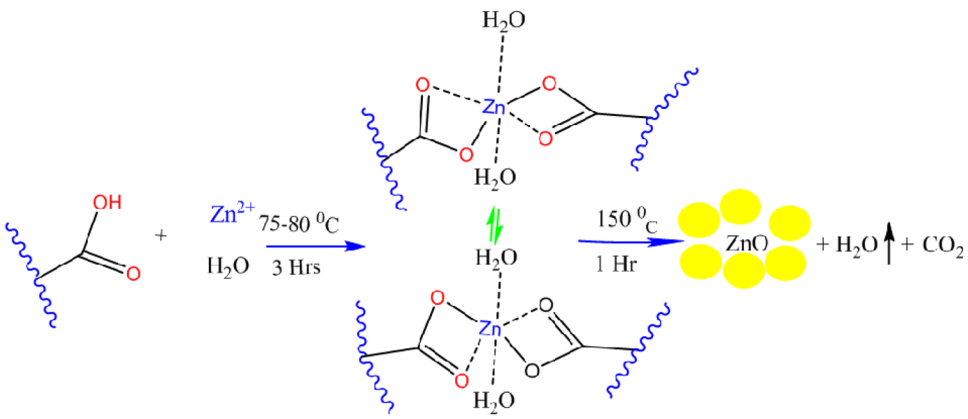

Fig. 4 A proposed mechanism for the formation of ZnO-NPs [55]

successfully applied in heavy crude oil cracking for reduction of dynamic viscosity of crude oil due to the presence of dipole water molecules. A simple and green method has been used by Kashale et al. [57] for the synthesis of TiO_2 nanoparticles, by reacting $TiCl_4$ with kitchen wastewater obtained from soaking Bengal gram beans (*Cicer arietinum* L.) extract. The morphology, specific surface area and pore size distribution of a synthesized TiO_2NP was investigated using XRD, Raman spectroscopy, TEM, TGA and BET surface area measurement system and applied to lithium ion battery. The Li-intercalation properties were evaluated using TiO_2NPs as anode in the half-cell configuration (Li/Bio-TiO_2). Interestingly, the green synthesized TiO_2NP displayed a good cyclability and retained 98% of its initial reversible capacity even after 60 galvanostatic cycles. In 2014, Kumar et al. [58] reported the synthesis of ZnONPs using an extract of Grape fruit. The ZnONPs were in the size range of 12–72 nm (TEM), and they show promising performance when used as an antioxidant and photocatalyst for degradation of methylene blue (> 56% efficiency for photocatalysis). They also proposed the reaction mechanism as shown in Fig. 4; the flavonoids/limonoids/carotenoid molecules of the plant have free OH/COOH, which can react with $ZnSO_4$ to form zinc flavonoids/limonoids/carotenoid complex. After completion of the reaction, the solution was centrifuged and dried in a hot air oven. During drying and calcining, conversion of zinc flavonoids/limonoids/carotenoid complex into ZnONPs takes place.

Nava et al. [59] used tomato, orange, grapefruit and lemon peels for the synthesis of ZnO nanoparticle, and they examine the activity for photocatalytic degradation of MB under UV irradiation. Accordingly, the sample prepared from grapefruit peel extract exhibits 77% degradation efficiency at 180 min, while the other ZnONPs prepared from orange, lemon, tomato peel extracts show a higher photocatalytic activity of 95%, 97% and 97% at 180 min, respectively. The rate constants (K) are reported to be 0.0078, 0.0162, 0.0176 and 0.0195 corresponding to grapefruit, orange, lemon, and tomato peel extracts, respectively. With these results, the sample synthesized with the tomato peel extract, have a higher K than the other samples due to a smaller particle size and a nearly monodispersed size distribution when compared with the other samples, which could provide a larger surface area for a quicker absorption and degradation of the MB molecules, resulting in a higher performance when compared to chemically synthesized commercially available NPs that only display a 37% degradation at 120 min. The average sizes of the synthesized nanoparticles characterized by TEM were 9.66, 12.55, 11.39 and 9.01 nm corresponding to grapefruit, orange, lemon, and tomato peel extract samples, respectively.

Greener synthesis of zinc oxide nanoparticles using 25% (w/v) of *Azadirachta indica* (Neem) leaf extract has been reported by Bhuyan et al. [60]. The biosynthesized ZnO nanoparticles, well characterized by TEM, EDX, and spectroscopic techniques and revealed spherical in shape with 9.6–25.5 nm particle size. Their studies on the antibacterial activity of the biosynthesized ZnO nanoparticles, using shake flask technique, revealed that the NPs were more active against the gram-positive bacteria; *Staphylococcus aureus* and *Streptococcus pyogenes* than against gram-negative bacteria; *Escherichia coli*. Further, it also exhibited photocatalytic activity under the UV light enhancing the degradation rate of methylene blue a major water pollutant released by the textile industries.

Pallela et al. synthesized CuO nano rod using *Asparagus racemosus* root extracts to test against pathogenic bacteria (gram positive and gram negative). The minimum inhibitory concentration of CuO nano rod was 6.25 µg/mL for both bacteria types. The zone of inhibition of CuO nano rod with 50 µg/mL concentration was found highest for *B. subtilus* (23.00 ± 0.63 followed by *S. aureus* (21.83 ± 0.75), *K. pheumonia* (20.00 ± 0.63), E. coli (19.83 ± 0.75), *A hydrophila* (19.00 ± 0.63), *F. fluorescens*, (18.83 ± 0.75), *Y. ruckeri* and *E. tard* (17.95 ± 0.46) [61]. Similarly, the author of this group synthesized CuONPs using *Aloe vera* leaf extracts for antibacterial activity against fish bacterial pathogens. They used 10–100 µg/mL of concentration range to evaluate the MIC of the NP. An increasing of zone of inhibition was observed above 20 µg/mL for all of the bacteria, while the sensitivity of *P. fluorescensis* was higher at lower concentrations (20–60 µg/mL) showing highest zone of inhibition when compared to *A. hydrophila* and *F. branchiophilum*. On the other hand, the sensitivity of *A. hydrophilais* was higher at high concentrations of CuONPs (60–100 µg/mL) with maximum zone of inhibition compared to other bacterial pathogens. However, CuONPs with 100 µg/mL concentration appears to be effective as there was no bacterial growth, with zones of inhibition for *A. hydrophila, P. fluorescens* and *F. branchiophilum* being 21, 19 and 17 mm, respectively using sulphafurazole as a positive control [62].

The available data on the green synthesis of some metal oxide nanoparticles mediated by different plant extracts, the particle size, their characterization and applications have been summarized in Table 1.

Table 1 Plant mediated synthesis of metal oxide nanoparticles

Plant	Plant part	NPs	Metal ion source	Size (nm)	Shape	Studied applications	Ref
Cynodon dactylon	Leaf	TiO_2	$Ti[(CH_3)_2CHO]_4$	13–34 (TEM)	Hexagonal	Antibacterial and anticancer	[63]
Azadirachta indica	Leaf	Mn_3O_4	$[Mn(CH_3COO)_4{\cdot}4H_2O]$	18.2 (XRD)	Spherical	Catalytic thermal decomposition of ammonium perchlorate (AP)	[64]
	Leaf	ZnO	$Zn(CH_3COO)_2{\cdot}2H_2O$	9.6–25.5 (TEM)	Hexagonal wurtzite	Antibacterial and photocatalytic applications	[60]
Moringa oleifera	Leaf	ZnO	$Zn(NO_3)_2{\cdot}6H_2O$	12.27–30.51	–	–	[65]
	Peel	CeO_2	$Ce(NO_3)_3{\cdot}6H_2O$	45 (HRTEM)	Spherical	Photocatalytic and antibacterial	[66]
Kalopanax pictus	Leaf	MnO_2	$KMnO_4$	19.2	Spherical	Degradation ability of dyes (congo red and safranin O)	[67]
Garlic Vine	Leaf	Fe_2O_3	$FeSO_4{\cdot}7H_2O$	18.22 (XRD)	Hexagonal	–	[68]
Ixora Coccinea	Leaf	ZnO	$Zn(CH_3COO)_2{\cdot}2H_2O$	145.1(DLS)	Hexagonal wurtzite	–	[69]
Artocarpus heterophyllus	Leaf	ZnO	$Zn(NO_3)_2{\cdot}6H_2O$	15–25(SEM)	Hexagonal wurtzite	Photocatalytic degradation of Rose Bengal dye	[70]
Anisochilus carnosus	Leaf	ZnO	$ZnNO_3$	30–40 (TEM)	Hexagonal wurtzite	Antibacterial and photocatalytic activities on methylene blue	[71]
Allium sativum	Bulb	ZnO	$Zn(NO_3)_2{\cdot}6H_2O$	14–70 (XRD)	Hexagonal wurtzite	Photodegradation of methylene blue	[72]
Petroselinum crispum	Leaf	ZnO	$Zn(NO_3)_2{\cdot}6H_2O$	14–70 (XRD)	Hexagonal wurtzite	Photodegradation of methylene blue	[72]
Artocarpus gomezianus	Fruits	ZnO	$Zn(NO_3)_3{\cdot}6H_2O$	11.53 (XRD)	Spherical, hexagonal wurtzite	Photocatalytic degradation of dye and antioxidant	[73]
Asparagus racemosus	Root	Fe_2O_3	$FeCl_3{\cdot}6H_2O$	30–40	Spherical	Photodegradation of methylene orange	[74]
Annona squamosal	Peel	TiO_2	$TiO(OH)_2$	23 ± 2 (TEM)	Spherical	–	[75]
Plectranthus amboinicus	Leaf	ZnO	$ZnNO_3$	50–180 (SEM)	Rod shape	Photocatalytic activity (methyl red)	[76]
Plantain peel	Peel	Fe_3O_4	$FeCl_3{\cdot}6H_2O$	< 50 (SEM)	Spherical	–	[77]
Saraca indica	Flower	SnO_2	$SnCl_4{\cdot}xH_2O$	2.1–4.1 (HRTEM)	Spherical	Antibacterial and antioxidant activities	[78]
Phyllanthus niruri	Leaf	ZnO	$ZnNO_3$	25.61 (SEM)	Hexagonal wurtzite	Photodegradation of methylene blue	[79]
Euphorbia Jatropa	Leaf	ZnO	$ZnNO_3$	15 (XRD)	Hexagonal shape	–	[80]
Calotropis gigantean	Leaf	ZnO	$Zn(CH_3COO)_2{\cdot}2H_2O$	10 (XRD)	Spherical	Nanofertilizers	[81]
Carica papaya	Leaf	CuO	$CuSO_4$	140 (DLS)	Rod shape	Photocatalytic dye degradation	[82]
Aspalathus linearis	Leaf	SnO_2	$SnCl_4{\cdot}5H_2O$	8.23 ± 0.12 (TEM)		Photocatalytic activity	[83]
Cassia fistula	Leaf	ZnO	$Zn(NO_3)_3{\cdot}6H_2O$	5–15 (TEM)	Hexagonal wurtzite	Photodegradative, antioxidant and antibacterial activities	[84]
Hibiscus Sabdariffa	Flower	CdO	$Cd(NO_3)_2{\cdot}4H_2O$	113 (SEM)	Cuboid shape	–	[85]
Agathosma betulina	Leaf	ZnO	$Zn(NO_3)_2{\cdot}6H_2O$	15.8 (TEM)	Quasi-spherical	–	[86]

Table 1 (continued)

Plant	Plant part	NPs	Metal ion source	Size (nm)	Shape	Studied applications	Ref
	Leaf	NiO	$NiCl_2{\cdot}6H_2O$	26.7 ± 0.4 (HRTEM)	Cubic	–	[87]
Poncirus trifoliate	Fruits	ZnO	$ZnNO_3$	21.12 (TEM)	Hexagonal wurtzite, spherical shape	Catalytic activity	[88]
Corymbia citriodora	Leaf	ZnO	$Zn(NO_3)_2{\cdot}6H_2O$)	64 (TEM)	Hexagonal wurtzite	Photocatalytic activity	[89]
Eucalyptus globulus	Leaf	ZnO	$(NO_3)_2{\cdot}6H_2O$	11.6 (TEM)	Spherical	Photocatalytic and antioxidant activity	[90]
Camellia sinensis (green tea)	Leaf	ZnO	$Zn(CH_3COO)_2{\cdot}2H_2O$	54.84 (XRD)	Hexagonal wurtzite	Supercapacitor applications	[91]
Eichhornia crassipes	Leaf	ZnO	$ZnNO_3$	32 ± 74	Spherical shape	–	[92]
Citrus paradise	Peel	ZnO	$ZnSO_4{\cdot}7H_2O$	12–72 (TEM)	Spherical	Photocatalytic degradation of methylene blue and antioxidant activity	[58]
Citrus sinensis	Leaf	Fe_2O_3	$Fe(NO_3)_3{\cdot}9H_2O$	60 (SEM)	Spherical	photocatalytic activity	[93]
Annona squamosal	Fruits	SnO_2	$SnCl_2{\cdot}2H_2O$	27.5 (TEM)	Spherical	Sytotoxicity against *hepatocellular carcinoma ell*	[94]
Physalis alkekengi	Shoot	ZnO	$ZnSO_4$	72.5 (TEM)	Triangular	Remediation of zinc-contaminated soils	[95]
Morinda citrifolia	Root	TiO_2	$TiO(OH)_2$	20.46–39.20	Spherical	*Larvicidal* activity against *Anopheles stephensi, Aedes aegypti and Culex quinquefasciatus*	[96]
Psidium guajava	Leaf	TiO_2	$TiO(OH)_2$	32.58 (FESEM)	Spherical	Antibacterial and antioxidant properties	[97]
Lycopersiconesculentum		ZnO	$ZnNO_3$	20–70 (DLS), 40–100 (TEM)	Spherical shape	Photovoltaic application	[98]
Abutilon indicum	Leaf	CuO	$Cu(NO_3)_2{\cdot}3H_2O$	16.78 (XRD)	*Hexagonal wurtzite*	Antimicrobial, antioxidant and photocatalytic dye degradation activities	[99]
Carissa edulis	Fruits	ZnO	$ZnNO_3$	50–55 (TEM)	Flower shape	Photocatalytic degradation of congo red	[100]
Peganum harmala	Seed	ZnO	$ZnNO_3$	40 (TEM)	Non-uniform shape	Removal of Cr(VI) from aqueous solution	[101]
Lemon	Fruits	ZnO	$ZnNO_3$	49.16 (HRTEM)	Hexagonal wurtzite	Photocatalytic dye degradation	[102]
Leucas aspera	Leaf	CeO_2	$Ce(NO_3)_3{\cdot}6H_2O$	4–13 (TEM)	Uniform microspheres	Photocatalytic and antibacterial	[103]
Cauliflower (Brassica oleracea)	Leaf	SnO_2	$SnCl_2{\cdot}2H_2O$	3.62–6.34 (TEM)	Quasi-spherical	Photocatalytic activities	[104]
Amorphophallus konjac	Tuber	ZnO	$Zn(CH_3COO)_2{\cdot}2H_2O$	19.7 (XRD)	Rice shaped	Solar cells	[105]
Catunaregam spinose	Root	SnO_2	$SnCl_2$	47 ± 2 (TEM)	Spherical	Photocatalytic degradation of diazo dye	[106]

Table 1 (continued)

Plant	Plant part	NPs	Metal ion source	Size (nm)	Shape	Studied applications	Ref
Persia Americana/ Avocado	Seed	SnO_2	$SnCl_2$	4 (XRD)	–	Degradation of phenolsulfonphthalein (phenol red).	[107]
Jatropha curcas	Leaf	TiO_2	$TiCl_4$	10–209 (FESEM)	Spherical	Tannery wastewater treatment	[108]
Eucalyptus globulus	Leaf	NiO	$NiNO_3{\cdot}6H_2O$	19 (XRD)	Pleomorphism	Antibacterial and anti-biofilm activity	[109]
Aloe vera	Leaf	α-Fe_2O_3	$FeCl_3{\cdot}6H_2O$	< 10	Hexagonal	Antibacterial and antibiofilm activities	[110]

2.3.2 Algae mediated biosynthesis of metal oxide nanoparticles

Algae are eukaryotic aquatic oxygenic photosynthetic organism which ranges from unicellular forms (ex. *Chlorella*) to multicellular ones (ex. Brown algae) but lack of basic plant structure like roots and, leaves [15, 111]. Microalgae attract special attention since they have the ability to bioremediate toxic metals, subsequently converting them to more amenable forms [15]. Macroalgae have different active metabolites like alkaloids, polyketides, cyclic peptide, polysaccharide, proteins, phlorotannins, diterpenoids, stereos, quinones, lipids and glycerol, which can be used for the synthesis of nanoparticles [112, 113]. The unusual optical, chemical, photoelectrochemical and electronic properties of the NPs received a great interest. 10–50 nm average size of *Ulva lactuca* seaweed mediated fabricated ZnONPs was tested for degradation of MB dye under direct sunlight irradiation, 90% MB degradation was achieved at the optimal initial dye concentration of 25 ppm irradiated in 120 min [114, 115].

The collected seaweeds were washed under running water to remove dirt, salt and other foreign materials and then soaked in deionized water. The washed algae or seaweed was allowed to dry, powdered and appropriate dried seaweed was soaked in deionized water for hours. The resulting extract was filtered using filter paper. Finally, a solution containing metal ion source salt was added to prepare the metal oxide nanoparticles as demonstrated in Fig. 5 below [116] (Table 2).

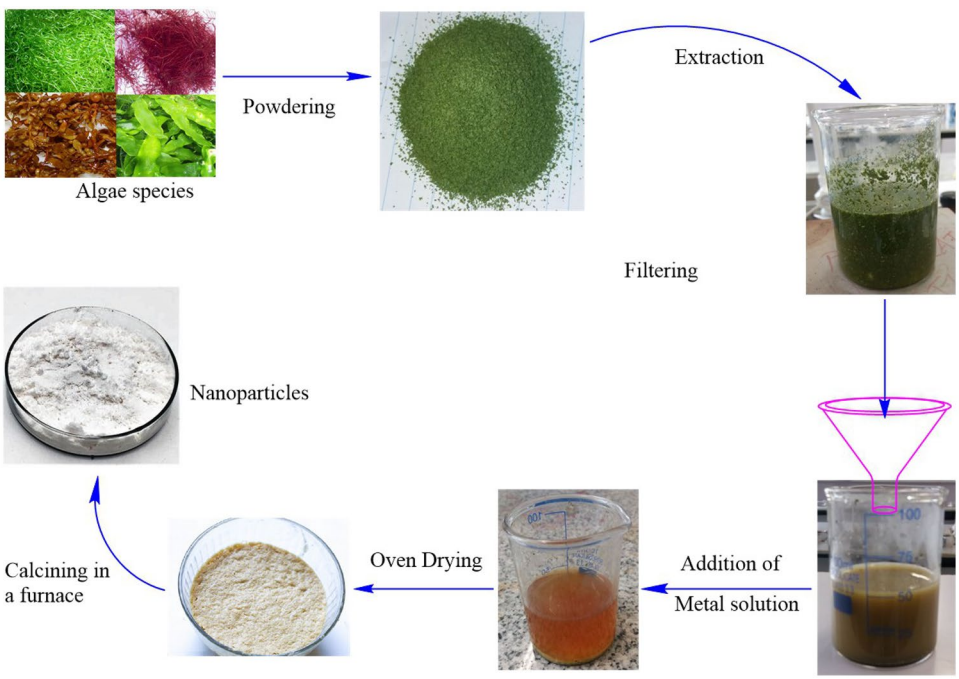

Fig. 5 Algae mediated synthesized of metal oxide nanoparticles

Table 2 Micro and macro algae mediated synthesis of metal oxide nanoparticle

Algae	NPs	Metal ion source	Size	Shape	Studied applications	Referencs
Sargassum muticum	ZnO	$Zn(CH_3COO)_2{\cdot}2H_2O$	30–57 (FESEM)	Hexagonal wurtzite	–	[117]
	Fe_3O_4	$FeCl_3$	18 ± 4 (TEM)	Cubic shapes	–	[118]
Bifurcaria bifurcata	CuO	$CuSO_4$	20.66 (TEM)	Spherical	Antimicrobial activity	[119]
Chlamydo-monas reinhardtii	ZnO	$Zn(CH_3COO)_2{\cdot}2H_2O$	21 (XRD)	Hexagonal wurtzite	Photocatalytic activity	[120]
Sargassum wightii	ZnO	ZnO_3	20–62	Spherical	*Larvicidal* and *Pupicidal* toxicity on A. *stephensi* and *H. armigera*.	[114]
Ulva lactuca	ZnO	$Zn(CH_3COO)_2$	10–50 (TEM)	Sponge-like asymmetrical shaped	Photocatalytic, antibiofilm and insecticidal activity	[115]
Gracilaria edulis	ZnO	ZnO_3	65–95 (FESEM)	Rod-shaped	Anticancer activity	[121]

2.3.3 Bacteria mediated biosynthesis of metal oxide nanoparticles

Among the milieu of natural resources, prokaryotic bacteria have been most extensively researched for the synthesis of metallic nanoparticles. One of the reasons for "bacterial preference" for nanoparticles synthesis is their relative ease of manipulation [41]. The bacterial cell reduces metal ions by use of specific reducing enzymes like NADH-dependent reductase or nitrate dependent reductase [122].

The major bacterial species used for the synthesis of metallic nanoparticles include *Actinobacter* sp., *Escherichia coli, Klebsiella pneumonia, Lactobacillus* spp., *Bacillus cereus, Corynebacterium* sp, and *Pseudomonas* sp. [15, 111]. The bacteria are known to synthesize metallic nanoparticles by either intracellular or extracellular mechanisms [123]. Even though bacteria-mediated nanoparticle biosynthesis is known to produce less toxic metal oxide nanoparticles, such as CuO, TiO_2, ZnO, and iron oxide, it involves fastidious cell culturing alongside difficulties in controlling the size distribution, shape and crystallinity of many metal oxide nanoparticles [44].

Kirthi et al. [124] synthesized TiO_2 nanoparticles using $TiO(OH)_2$ as a precursor, and the bacterium, *Bacillus subtilis* as a reducing agent. The synthesized nanoparticles were confirmed as TiO_2 nanoparticle. The morphological characteristics of TiO_2 were found to be spherical oval in shape, individual nanoparticles as well as a few aggregates had the size of 66–77 nm.

Khan and Fulekar [125] reported biosynthesis of TiO_2 using *Bacillus Amyloliquefaciens* as a capping agent. The synthesized TiO_2NPs revealed the formation of spherical nanoparticles with a size range of 22.11–97.28 nm. Photocatalytic degradation of Reactive Red 31 was tested by the nanoparticle using platinum doped TiO_2 which showed the highest potential (90.98%) in RR31 degradation as compared to undoped (75.83%). Similarly, Ordernes-aenishanslins et al. [126] produce TiO_2NPs using a culture of 200 µL of *Bacillus mycoides* grown overnight by adding 40 mL of a 25 mM titanyl hydroxide solution and incubated at 37 °C for 24 h with constant shaking. The isolate was able to biotransform the precursor into its nanostructured, 40–60 nm size and spherical shape. A possible mechanism for TiO_2 biosynthesis using titanyl hydroxide as a precursor and an unknown organic molecule from *B. mycoides* (X) is proposed in Fig. 6 below. Works reported by researchers on bacteria mediated green synthesis of metal oxide NPs has been summarized in Table 3.

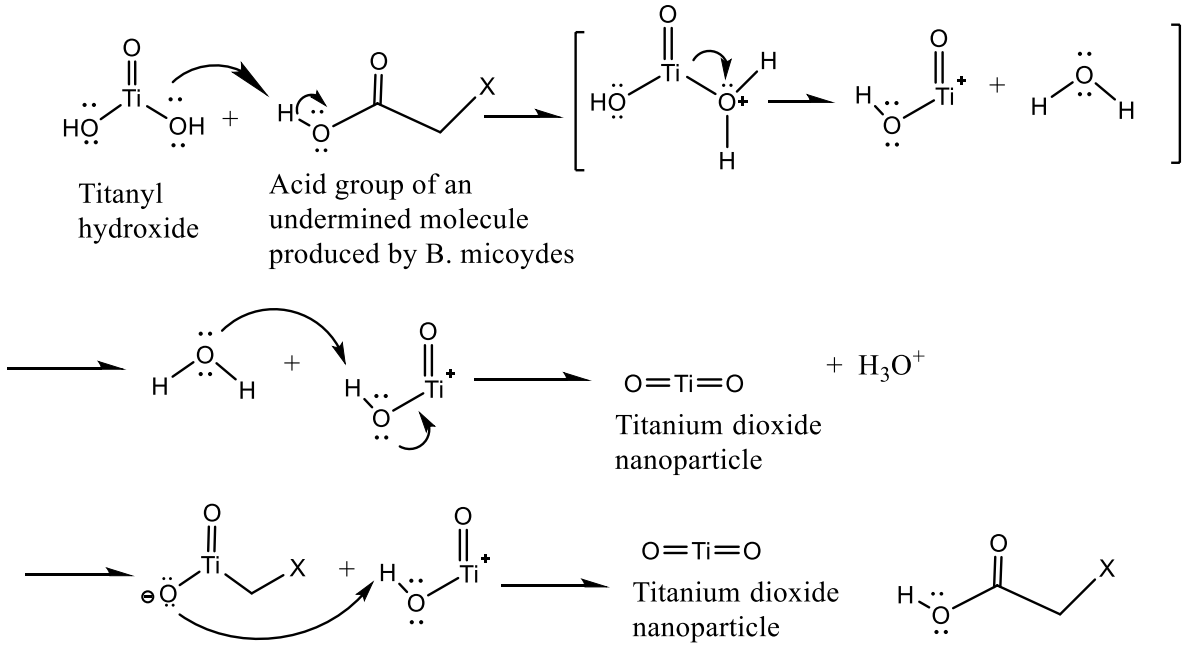

Fig. 6 Possible mechanism for biotransformation of titanyl hydroxide to titanium dioxide nanoparticles. The dehydration reaction would be mediated by an acidic group present in an "unknown" component of the extracellular matrix of *B. mycoides* that could have a key role in biotransformation [126]

Table 3 Bacteria mediated synthesis of metal oxide nanoparticles

Bacteria species	NPs	Metal ion source	Size	Shape	Studied application	References
Aeromonas hydrophila	ZnO		57.72 (AFM)	Spherical	Antibacterial and anti-fungi activity	[127]
Aeromonas hydrophila	TiO_2	$TiO(OH)_2$	28–54 (FESEM)	Spherical	Antibacterial activity	[128]
Rhodococcus pyridinivorans NT2	ZnO	$ZnSO_4{\cdot}H_2O$	100–120 (FESEM, TEM)	Hexagonal	Photocatalytic activity on malachite green	[129]
Bacillus subtilis	TiO_2	$TiO(OH)_2$	66–77 (SEM)	Spherical	–	[124]
Bacillus subtilis	TiO_2	K_2TiF_6	10–30 (TEM)	Spherical	Photocatalytic activity on aquatic biofilm	[130]
Bacillus licheniformis MTCC 9555	ZnO	$Zn(O_2CCH_3)_2{\cdot}2H_2O$	–	Hexagonal wurtzite	Photocatalytic activity	[131]
Bacillus amyloliquefaciens	TiO_2	$TiOSO_4$	22.11–97.28 (TEM), 15.23–87.6 (XRD)	Spherical	Photocatalytic activity for the degradation of a sulfonated textile dye Reactive Red 31	[125]
Microbacterium sp. MRS-1	NiO	$NiSO_4$	100–500 (AFM)	Spherical flower	Bioremediation of nickel electroplating industrial effluent	[132]
Micrococcus lylae, Micrococcus aloeverae, Cellulosimicrobium sp.	TiO_2	$TiO(OH)_2$	14–17 (TEM)	Spherical	Wastewater remediation	[133]
Bacillus mycoides	TiO_2	$TiO(OH)_2$	40–60 (TEM)	Spherical	Solar cells	[126]

2.3.4 Fungi mediated biosynthesis of metal oxide nanoparticles

In recent years, fungi, among several groups of living organisms, have also been used as a better mediator for the biosynthesis of metal oxide nanoparticles (NPs). The green fabrication of NPs using different strains of fungi is much interest since this group of organisms is directly or indirectly dependent on metals for their growth, metabolism, and differentiation. The use of eukaryotic organisms of fungi offers considerable promise for large-scale metal/metal oxide NPs production since the enzymes that are secreted by the fungi represent an essential ingredient for the biosynthesis of metal and metal oxide NPs [134, 135]. A biologically induced method to synthesize titanium dioxide NPs using *Aspergillus flavus* as a reducing and capping agent show that the NPs were primarily composed of aggregate nanosized particles with average particle sizes ranging from 62 to 74 nm. The NPs synthesized using this technique was evaluated for antimicrobial activity against five pathogenic bacterial strains viz. *S. aureaus, E coli, P. aeruginosa, K. pneumonia, B. subtills*. Among the bacterial strains tested, TiO_2NPs showed superior antimicrobial activity against *E. coli* (MTCC-1721). Rajakumar et al. [136] demonstrated the fabrication of TiO_2NP from fungus using various precursor salts (sulfate, nitrate, chloride, and oxide salts). The product of this study revealed 0.1 mM precursor salt concentration, 72 h of incubation at pH 5.5 and 28 °C resulted in more nanoparticle yield. The advantages of fungal biosynthesis of nanoparticles is that fungi possess very high intracellular metal uptake capacities and a large number of enzymes are produced per unit biomass. Extracellular enzymes secreted by fungi such as reductases have facilitated the formulation of metal nanoparticles with different chemical compositions [44]. Recently, fungus mediated metal oxide nanoparticles have been used as nano-nutrient fertilizer, delivered either by soil or root application. The small particle size of the nanoparticle base nutrient up take by roots is quite higher than the conventionally fertilizer applied through the soil. To enhance solar light absorption by plant leaves to boost plant photosynthesis, fungus originated titanium dioxide and magnesium oxide nanoparticles were used because of their photocatalytic activity and essential part of pigment chlorophyll structures, respectively. *Aspergillus flavus* mediated synthesized titanium dioxide nanoparticles (12–15 nm) enhances chlorophyll content in the mung bean plant leaves by 46.4% and for plant fertilizer purpose [137, 138], similarly, zinc oxide nanoparticles have been synthesized using *Aspergillus fumigatus* TFR [139]. Fungal spores of *Fusarium oxysporum* have been used for the synthesis of novel tertiary oxide nanostructures of barium titanate ($BaTiO_3$) and bismuth oxide (Bi_2O_3) [44]. Ibrahem et al. [140] synthesis zinc oxide nanoparticles (ZnONPs) using biological methods as eco-friendly using *Aspergillus niger* filtrate in the extracellular synthesis, then characterized by UV–Vis Spectrophotometer and Scanning Electron Microscopy (SEM) appear as spherical in shape and 41–75 nm particle size. Furthermore, the biological synthesized ZnONPs was tested against isolated pathogen microbes; *Staphylococcus aureus* and *Escherichia coli*.

The works reported by researchers on the fungus mediated green synthesis of metal oxide NPs has been summarized in Table 4.

Table 4 Fungus mediated synthesis of metal oxide nanoparticles

Fungi species	NPs	Metal ion source	Size	Shape	Studied application	References
Aspergillus flavus TFR 7	TiO_2	(Bulk TiO_2)	18 (DLS), 12–15 (TEM)	–	Plant nutrient fertilizer to enhance crop production	[137]
Aspergillus flavus	TiO_2	TiO_2	62–74 (SEM)	Spherical	Activity against pathogenic bacteria	[136]
Pichia fermentans JA2	ZnO	ZnO	–	Smooth and elongated	Antimicrobial	[141]
Aspergillus fumigatus TFR-8	ZnO	$ZnNO_3$	54.8–82.6 (SEM), 29 (XRD)	spherical	Enhance phosphorous mobilizing enzymes and nanoinduced gum production.	[139]
Aspergillus niger	CeO_2	$CeCl_3{\cdot}7H_2O$	5–20 (TEM)	Cubic and spherical	Antibacterial and l*arvicidal* activities	[142]
Cladosporium cladosporioides	NiO	$NiCl_2$	9.9	Cubic	Energy storage	[143]
Hypocrea lixii	NiO	$NiCl_2{\cdot}6H_2O$	1.25 & 3.8 (SEM)	Spherical	Removal of toxic metals from polluted sites	[144]
Humicola sp	CeO_2	$Ce(NO_3)_3{\cdot}6H_2O$	16 (TEM)	Spherical	–	[145]

3 Characterization of metal oxide nanoparticles

The distinct physicochemical properties of the nanomaterials such as; size, surface properties, shape, composition, molecular weight, identity, purity, stability, and solubility, are critical for the interaction of the nanomaterials for different applications [146].

In order to characterize nanoparticles for the aforementioned properties, several state art instruments are present and the most commonly used techniques are; Dynamic light scattering (DLS), Electron microscopy (TEM, SEM), Atomic force microscopy (AFM) are used to measured morphology (shape, size), XRD for topography (surface) analysis, UV–visible spectroscopy is used to measured optical properties and band gap usually in the range of 200–800 nm, DLS and Electron dispersive X-ray spectroscopy (EDX) are exercised to analyses size distribution and dispersed in liquid and elemental composition of the NPs respectively, FTIR is used to determine

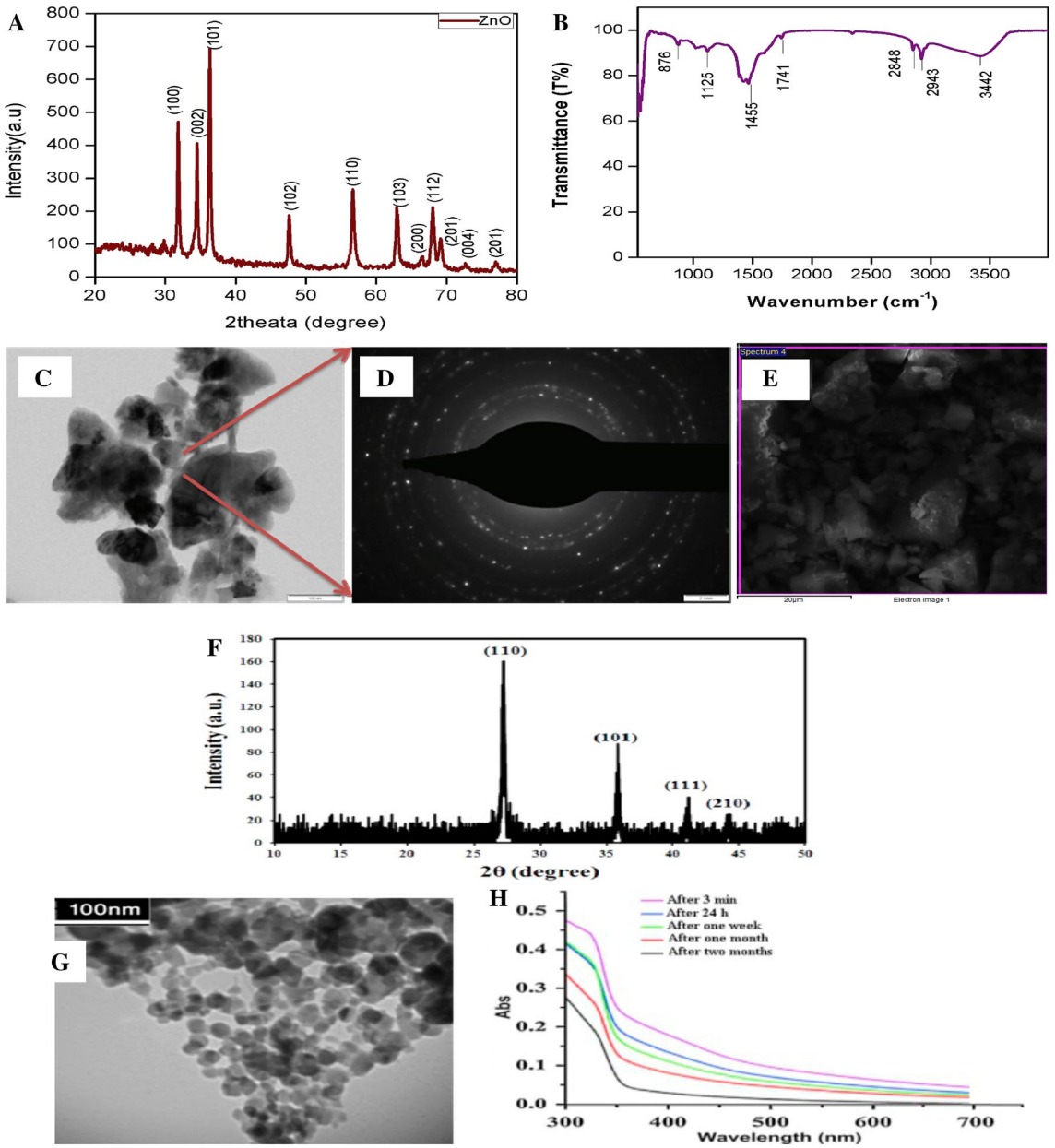

Fig. 7 XRD peak (**a**), FTIR spectra (**b**), TEM image (**c**), **d** SAED pattern, SEM image (**e**) of *Glycosmis pentaphylla* leaf extract mediated synthesis of ZnO and XRD peak (**f**), TEM image (**g**), UV–Vis spectrum (**h**) of *Euphorbia heteradena Jaub* root mediated synthesis of TiO_2 nanoparticle [51, 148]. © Elsevier, reproduced with permission

the nature of functional groups of metabolites present on the surface of the NPs [40]. The spectrum and images characterization results of the plant mediated synthesis of ZnO and TiO_2 nanoparticles is shown in Fig. 7. The FTIR spectrum of zinc oxide nanoparticles synthesized from *Costus pictus* leaf extracts absorbs at 441.51–665.50 cm^{-1}. The O–H stretch appears in the spectrum as a very broad band extending at 3372.37 cm^{-1}. This very broad O–H stretch band is observed with a C=O peak, which almost certainly indicates that the compound is an aliphatic carboxylic acid [147]. FTIR spectrum of *Jacaranda mimosifolia* flowers (JMFs) extract synthesized ZnONPs exhibits a broad peak at 3373.12 cm^{-1} corresponding to O–H stretching vibration whereas the peaks at 2942.29 cm^{-1}, 2830.04 cm^{-1}, 1647.43 cm^{-1} and 1031.62 cm^{-1} correspond to C–H stretching, carbonyl group (C=O) and C–H bending, respectively. The spectra of ZnONPs synthesized with and without JMFs extract shows characteristic peaks of Zn–O stretching at 745.54 cm^{-1} and 779.45 cm^{-1}, respectively confirming the formation of ZnONPs [54].

Sargassum muticum assisted synthesis of ZnONPs by Mahdavi et al. [117] was confirmed via FTIR spectrum, a signal at 441 cm^{-1}corresponded to the stretch band of zinc and oxygen, XRD characteristic of the nanoparticles confirms hexagonal wurtzite structure, and particle size distribution measured using SEM was 30–57 nm. Similarly, *Arabic gum* mediated synthesized of ZnONPs show a peak in the region between 400 and 600 cm^{-1} which is allotted to Zn–O vibration. The UV–Vis measurement reveals a characteristic absorption peak of ZnO at a wavelength of 378 nm. The SEM image shows the particle size and external morphology of the ZnO nanoparticles that was calcined at 500 °C for 4 h, fairly uniform spherical shape and narrow size distributions in the average size of 10 nm. [149]. Fe_2O_3 NPs synthesized by *Psoralea corylifolia* seeds extract reducing agent confirmed the fabrication of the NPs at 526 and 450 cm^{-1} indicated the presence of Fe–O bond vibrations in the FTIR spectrum. The morphologies of nanoparticles were investigated by SEM and TEM and have rod-like or uneven shapes and spherical, hexagonal and cubic in shape respectively, the average size of nanoparticles was estimated to be 39 nm according to the Scherrer equation [150]. Synthesis of Fe_2O_3 using *Emblica officinalis* fruit extract reported by Malarkodi et al. [151] also characterized by FTIR and spectral bands at 536 and 454 cm^{-1} were observed due to Fe–O stretching. The UV–visible diffuse reflectance spectrum consisted of the strong absorption of Fe_2O_3 was found at 530 nm. The band gap energy was found to vary from 1.97 to 2.05 eV. SEM images coupled with TEM revealed that the aggregation of rod-shaped of Fe_2O_3 crystalline with a diameter ranging 20–100 nm. The size of the nanoparticles depends on the calcination temperature and the band gap energy will vary little due to the sample size. Usually, the smaller the size of the particle, the greater should be the band gap [71] as illustrated in Table 5.

Table 5 Characterization of selected biosynthesized metal oxide nanoparticles

NPs	UV–Vis absorbance peak (nm)	FTIR spectrum of NPs (cm^{-1})	Size (nm)	Band gap energy (eV)	References
CeO_2	296	468	–	3.28	[145] [142]
TiO_2	380	450–700	40–60	3.27	[126]
	379	–	10–30	3.273	[130]
	403	433	20–40	3.21	[152]
ZnO	377	393	22	3.29	[153]
	353	410	10	3.34	[154]
	377	429–490	9.6–25.5	3.87	[60]
	322 and 334	530	50–90	3.38	[98]
	400	445	20–30	3.46	[155]
	378	400 and 600	10	–	[149]
Fe_3O_4	402 and 415	535 and 307	17–25	–	[118]
	–	579	14	–	[156]
Fe_2O_3	378	618.88	13.82–15.45	2.84	[68]
	–	500	29	–	[157]
HgO	243	471, 650	2–4	2.48	[158]
Dy_2O_3	285, 358, 477	591	35–45	5.45	[159]

The elemental composition of green synthesis of Co_3O_4 nanoparticles via *Aspalathus linearis* leaf extract was deduced using EDS spectrum. The average Co/O atomic ratio deduced from the EDS studies is found 2.91/3.95, which is, within the bar error, consistent with the theoretical value of ¾, that is, Co_3O_4 and not CoO neither Co_2O_3 nor $Co(OH)_2$. No other element has been detected so far, which indicating the chemical purity of the Co_3O_4 nanoparticles following the preparation and final filtration protocol [160].

4 Application of metal oxide nanoparticles for water treatment

Conventional disinfection methods such as chlorination, ultraviolet, and ozonation, are essential steps in centralized water treatment to control microbial pathogens and waterborne epidemics. Even though, they are effective to disinfect wastewater, the powerful oxidants may react with natural organic matter (NOM) to form a wide range of disinfection byproducts (DBP), some of which have been identified as carcinogenic [161].

Furthermore, the survival of some pathogens, such as *Cryptosporidium* and *Giardia* to the conventional disinfectants requires extremely high disinfectant dosage, leading to the aggravated DBP formation [162]. Ozonation of waters that contain NOM and bromide leads to the formation of hypobromous acid (HOBr), hypobromide ion (OBr^-), bromate and brominated organic byproducts. Ozonation of bromide-containing water can produce brominated DBPs including bromate (BrO_3^-), bromoform ($CHBr_3$), bromoacetic acids (BAA), dibromoacetone (DBA) and dibromoacetonitrile (DBAN), and some of these inorganic and organic byproducts are potential carcinogens. Therefore, there is an urgent need to reevaluate conventional disinfection methods and to consider innovative approaches that enhance the reliability and robustness of disinfection while avoiding DBP formation [162–164]. In addition to the modification of existing treatment processes such as enhanced coagulation to remove NOM, novel disinfection approaches have been explored [165].

Nanotechnology has the potential to advance water and wastewater treatment by improving treatment efficiency. There are several classes of nanomaterials that are being evaluated as materials for water purification which have a broad range of physicochemical properties which make them attractive for water purification [166]. The application of nanoparticles such as fullerene based nanomaterials, ZnO nanoparticles, photocatalytic nanoparticles (e.g., TiO_2) for disinfection has captured significant interest [161].

Nano adsorbents are effectively used in the removal of organic compounds, metal ions and their selectivity toward particular pollutants can be increased by functionalization. Nanoscale metal oxides, such as titanium dioxides, iron oxides, zinc oxides, alumina, etc., have been explored as low-cost, effective adsorbent for water treatment offering a more cost-efficient remediation technology due to their size and adsorption efficiency [167].

4.1 Removal of heavy metals

Heavy metal pollution of wastewater is one of the most vulnerable environmental problems throughout the world. Water contamination with toxic metal ions such as; Hg(II), Pb(II), Cr(III), Cr(VI), Ni(II), Co(II), Cu(II), Cd(II), Ag(I), As(V) and As(III) becomes public health and environmental challenges. Due to their serious health and environmental concerns, thus, there is a need to discover new and effective methods for their removal from water and wastewater. A number of studies have explored to the nanoparticles for adsorption of heavy metals, owing to the simplicity of modifying their surface functionality and their high surface area to volume ratio for enhanced adsorption capacity, efficiency and reuse [154, 168].

Srivastava et al. [169] revealed that ZnO nanoparticles have a high removal efficiency for Cd(II) using 20 mg/L of adsorbent dose, the removal efficiency was ~ 55% and on increasing the dose to 200 mg/L, a 92% removal of Cd(II) within 1 h of contact time was occur. Thus, then—ZnO nanoparticle could be successfully used for the removal of Cd from effluents.

Synthesized iron oxide nanoparticles using *tangerine* peel extract of spherical shape in the average size 50 nm worked by Ehrampoush et al. [170] investigated for removal of Cd(II) from wastewater. The peel extract of Fe_2O_3 nanoparticle shows effective removal of cadmium ions almost 90% occurred at pH of 4 and the adsorbent dose of 0.4 g/100 mL in 90 min contact time.

Peganum harmala seed extract mediated ZnO nanoparticles was synthesized by Fazlzadeh et al. [101]. The authors offered the nanoparticle for Cr(VI) removal

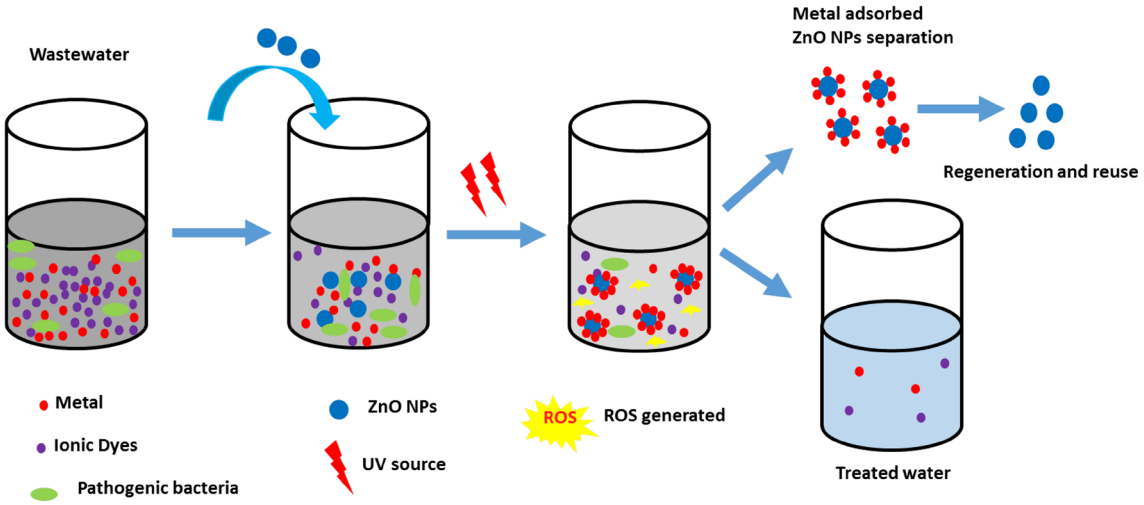

Fig. 8 Schematic representation of how ZnONPs can be used for systematic decontamination of wastewater containing metals, dyes, and microbes [171]. © John Wiley and Sons, reproduced with permission

from wastewater and it shows 97.59% removal efficiency at pH of 2, 1000 mg/L initial concentration, and 2 g/L load of the NPs in 30 min. Somu and Paul [171], studied casein based biogenic-synthesis of zinc oxide nanoparticles simultaneously to decontaminate heavy metals, dyes, and pathogenic microbes from wastewater. The NPs show maximum adsorption efficiency of 85.63% and 71.23% for Cd(II) and Co(II) respectively at pH of 7.0 and 95.35% for Pb(II) at pH of 8.0. Whereas, the degradation of the dyes was 93.58% for MB at pH of 7.0 and 94.72% for CR at pH of 6.0. The reusability of the ZnONPs was assessed by repeating adsorption–desorption processes five times and loaded ZnONPs after five cycles led to an adsorption loss of only 10–12% for both dyes and metals. Moreover, the NPs confirmed highest antibacterial potential for *Escherichia coli* in the presence of metals and dyes. As it is demonstrated in Fig. 8, when ZnONPs were applied to contaminated water with metals, dyes, and microbes, metals were adsorbed on ZnONPs surface. Dyes were also adsorbed on ZnONPs surface and photodegraded, mediated by UV irradiation through ROS generation. Bacteria were further inactivated by internalization of ZnONPs via ROS mediated oxidative stress. The used ZnONPs was finally regenerated for further reuse.

Calotropis procera latex mediated green synthesis of cupric oxide nanoparticles (CuONPs) was investigated its application for removal of Cr(VI) from aqueous solutions. The initial concentration of Cr(VI) and pH used for the experiment was 5 mg/L and 2.0 respectively. It was observed that the removal efficiency of CuONPs was 99.99% at the adsorbent dose of 18.84 g/L, but the nanoparticle which synthesized traditionally exhibits only 53% removal efficiency with the same amount of adsorbent dose. The adsorbent was successfully regenerated and reused up to five consecutive cycles without significant loss in removal capacity [172].

TiO_2 nanoparticle synthesized via a sol–gel method in the range of 19.29–26.72 nm, calcined at 400 °C was investigated for removal of Cd(II) from wastewater. The adsorption rate of cadmium ions was very fast in the first 30 min, and the adsorption equilibrium was achieved after 180 min and maximum adsorption capacity of Cd(II) is found to be 29.28 mg/g at pH of 6 [173] (Table 6).

Table 6 Removal of pollutants using bioinspired synthesized metal oxide nanoparticles

Plant/microorganism	NPs	Removal target	Initial conc. (mg/L)	Dose NPs (g/L)	Contact time (min)	pH	Removal efficiency (%)	Adsorption capacity (mg/g)	References
Peganum harmala, seed	ZnO	Cr(VI)	1000	2	30	2	97.59	74.67	[101]
Microbac-terium sp	NiO	Ni(II)	–	2.172	120 h	7	95	–	[132]
Jatropha curcas, leave	TiO_2	Cr(VI)	–	–	–	8.2	76.48	–	[108]
Mushroom	Fe_3O_4	Cr(VI)	200	12	240	3	73.88		[174]
Emblicao fficinallis	ZnO	As(III)	0.002	2.5	60	5	96.7		[175]
Ananas comosus, peel	Fe_3O_4	Cd(II)	60	0.1	10	6	96.1	49.1	[176]
Zingiber zerumbet	ZnO	Pb(II)	25	0.1	60	5	93	19.65	[154]
Tangerine peel	Fe_2O_3	Cd(II)	15	0.4	90	4	88.7	–	[170]
Casein	ZnO	Cd(II)	500	2	30	7	85.63	156.74	[171]
		Pd(II)	500	2	30	8	95.35	194.93	[171]
		Co(II)	500	2	30	7	71.23	67.93	[171]
Calotropis procera	CuO	Cr(VI)	5	18.84	120	2	99.99		[172]
A. Vera	α-Fe_2O_3	As(V)	2–30	0.5	–	6–8	–	38.48	[177]

4.2 Fluoride removal

Fluoride contamination of drinking water is one of the most serious health problems worldwide. An excessive fluoride intake leads to the loss of calcium from the tooth matrix, causing cavity formation, and ultimately leads to dental fluorosis followed by skeletal fluorosis after prolonged exposure. The increased surface area of the metal oxide nanoparticles highly favored for fluoride adsorption. Their high adsorption capacity, non-toxic nature, limited solubility in water and good desorption potential makes metal oxide nanoparticles a material of choice [178].

A number of magnetic nanoparticles such as Ce–Ti@Fe_3O_4 and Fe_3O_4@$Al(OH)_3$ are used for fluoride removal from contaminated water due to their large surface area, high reactivity, specificity, self-assembly, and recyclability. The former one shows a maximum adsorption capacity of 91.04 mg/g at pH of 7 and also showed a fast adsorption rate. The author also observed that it can be used for 5 cycles without significant loss of adsorption capacity. Composite Fe_3O_4@$Al(OH)_3$ nanoparticles, which combines the advantages of magnetic separation and aluminum oxide has a high affinity towards fluoride [179]. Similarly, Chai et al. [180] fabricated sulfate-doped Fe_3O_4/Al_2O_3 nanoparticles with magnetic separability for fluoride removal from drinking water. Nearly 90% adsorption can be achieved within 20 min and only 10–15% additional removal occurred in 8 h. The adsorption capacity of this nano-adsorbent for fluoride by two-site Langmuir model was 70.4 mg/g at pH 7.0. Moreover, this nano-adsorbent performed well over a considerable wide pH range of 4–10, and the fluoride removal efficiencies reached up to 90% and 70% throughout the pH range with initial fluoride concentrations of 10 mg/L and 50 mg/L, respectively. Silveira et al. [45] Synthesized FeONPs using *Moringa oleifera* leaf extract as a template for fluoride ion adsorption from wastewater and the study revealed that fluoride ion adsorption was favorable with maximum adsorption at pH of 7. Adsorption kinetics test showed that the equilibrium was reached in 40 min with an adsorption potential of 1.40 mg/g. The regeneration process showed that FeONPs is possible to reuse three times in the fluoride ion adsorption process. As a result of its adsorption capabilities and the shortest contact time to achieve equilibrium, the synthesized nanoparticles in their work is highly promising material for fluoride ion removal. Kumari and Khan [181] synthesized 51.48 nm of Fe_3O_4 using *Simmondsia Chinensis (*jojoba) defatted meal for defluoridation application from drinking water. The NPs was impregnated on to polyurethane foam (PUF) and made into tea infusion bags. The percentage F^- removal increased with increasing pH up to 5 and 6 for Fe_3O_4 NPs-PUF. But the F^- removal percentage decreases in the pH range of 5.0–9.0 for Fe_3O_4 NPs-PUF. In acidic pH conditions, the formation of hydrofluoric acid (HF) is responsible for the reduction of F^- adsorption but under alkaline conditions, F^- removal declined because of the competition between F^- ions and hydroxyl ions for the active surface sites. The adsorption of F^- ions reduced as the initial F^- concentration increased. The percent fluoride removal was found to be 93% at a contact time of 80 min. The Fe_3O_4 NPs-PUF displayed a higher water defluoridation capacity of 34.48 mg/g of F^-. TiO_2 nanoparticle was synthesized using a metal resistant *Bacillus* NARW11 species. The microbial synthesized TiO_2 nanoparticles were

tested for removal of F^- solutions which was treated with different dosages of TiO_2 nanoparticles having different phases (0.2–1.2 g/200 mL) to the equilibrium time for adsorbate concentration of 0.5–4 mg/L. The results revealed that increase in adsorbent dosage increased the percent removal and either reached a constant value or showed saturation after a particular dosage level. The more adequate adsorbent dosages for native, anatase, rutile and anatase mix rutile phase TiO_2 nanoparticles were found to be 0.6 g/200 mL. Native, anatase, anatase mix rutile and rutile phase TiO_2 nanoparticles showed the maximum F^- removal of more than 90% in the pH range of 2–4 for the initial adsorbate concentration of 0.5 mg/L in 80 min contact time [182].

4.3 Water disinfection from microbes

Microbial contamination of water is a public health concern because it causes numerous diseases and some aesthetic problems such as malodor in water. Organisms such as *Escherichia coli, Shigella* spp., *Salmonella* spp., *Vibrio* spp., and *Cryptosporidiu*m are known to be transmitted by water and cause ill health in communities consuming water contaminated by bacteria. Nanomaterials are excellent adsorbents, catalysts and sensors due to their large specific surface area and high reactivity. Several natural and engineering nanomaterials have also been shown to have strong antimicrobial properties [183].

Magnetic nanoparticles with poly allylamine hydrochloride (PAAH) stabilization were studied to determine their efficiency in removal pathogenic bacteria through electrostatic interaction and magnet capture from drinking water. High removal efficiency was achieved for four main pathogenic species, as *Escherichia*, *Acinetobacter*, *Pseudomonas,* and *Bacillus*, and the results showed high bacteria removal efficiency (99.48%) and the total bacteria residual counts was as low as 78 CFU/mL, which met the drinking water standard of WHO (< 100 CFU/mL) [184].

Mostafaii et al. [185] investigated the removal of total coliform bacteria using ZnONPs from the effluent of municipal wastewater. Different concentrations of ZnONPs in different reaction time and dose was tested on the removal efficiency of total coliform bacteria (0.3, 0.5, 0.7, 0.9 and 1.1 g/L) in 20, 40, 60 and 90 min reaction time. A load of 0.3 g/L of the nanoparticle in 20–90 min shows 96% removal efficiency, a dose of 0.5 g/L shows 75–98.66% removal efficiency in 20–90 min, a concentration of 0.7 g/L it shows 65% removal efficiency in 20 min and reached 99.4% in 90 min. Finally, high concentration of 1.1 g/L of ZnO in 90 min removed 100% of the total coliform bacteria from the municipal effluents. Novel microbial synthesized of ZnO nanoparticles using *Aeromonas hydrophila* in the size of 57.72 nm was tested against pathogenic bacteria. The well diffusion experiments were performed against the *A. hydrophila, E. coli, S. aureus, P. aeruginosa, E. faecalis, S. pyogenes, A. flavus, A. niger* and *C. albicans*. The maximum zone of inhibition was observed in the ZnONPs (25 µg/mL against *P.aeruginosa* (22 ± 1.8 mm) and *A. flavus* (19 ± 1.0 mm). The biosynthesized ZnO nanoparticle shows the minimum inhibitory concentration for *A. hydrophila, E. coli, E. faecalis, C. albicans* at 1.2, 1.2, 1.5, 0.9 µg/mL^{-1} respectively [127]. Hexagonal structure of ZnONPs synthesized via *Bauhinia tomentosa* leaf extract as bioreducing agent in an average size of 22–29 nm was reported. The antibacterial potential of the bioinspired NP was tested against *B. subtilis*, *S. aureus, P. aeruginosa,* and *E. coli*. The bactericidal effect of ZnONPs was found higher for gram-negative bacteria than gram-positive bacteria due to the difference in the structural composition of gram-positive and gram-negative bacteria. The plant extract-derived ZnONPs showed a significant zone of inhibition for *P. aeruginosa* (20.3 mm) and *E. coli* (19.8 mm), whereas the zone of inhibition for *B. subtilis* (8.1 mm) and *S. aureus* (10.7 mm) was less [186]. The interaction of ZnONP with food borne pathogens also showed a MICs of 80 µg/mL & 100 µg/mL for *E. coli* DH5α & *S. aureus* 5021 respectively, and the growth of the bacteria with treatment of bactericidal concentrations of ZnONP significantly retarded [187]. Green synthesis of copper oxide nanoparticles using aqueous leaf extract of *Origanum vulgare*, inhibits the cyanobacteria *Microcystis aeruginosa* which are commonly found in the eutrophic freshwater, create extensive secondary metabolites which are harmful to human and animal health. Copper oxide nanoparticles inhibited the growth of the colonial *Microcystis aeruginosa* nearly 89.7% with load of 50 mg/L NP and decreases to 62.6% in low concentration, 25 mg/L [188].

4.4 Photocatalytic activity of metal oxide nanoparticles

Photocatalysis refers to the acceleration of the rate of chemical reactions (oxidation/reduction) brought about by the activation of a catalyst, usually a semiconductor oxide and ultraviolet (UV) or visible irradiation [189]. Light and a catalyst are necessary to bring about or to accelerate a chemical transformation [190]. Organic pollutants such as a textile dye, pesticide, pharmaceutical waste, exist widely in wastewater, which are very harmful to the aquatic and terrestrial ecosystems. They are toxic because of their highly polar and persistent to environmental degradation processes and can result in serious bioaccumulation in the environment which will have a long half-life and the only trace can lead to biological variation [191]. Thus, there is a need for a new generation for wastewater treatment system that is environmentally friendly and can

minimize the associated human health and environmental. Among the new generations of wastewater treatment the technologies heterogeneous photocatalysis with an oxide semiconductor (nanoparticle) appears to be an attractive pre-treatment option to enhance the degradation of organic contaminants, as well as the biodegradability of the wastewater for further downstream treatments [192, 193].

Cassia fistula leaves mediated synthesis of ZnO nanoparticle shows photodegradation of methylene blue with an efficiency of 96.26–98.71% in the pH range of 2–4 of methylene blue dye solution [84]. Jayaseelan et al. [127] also confirmed that jackfruit (*Artocarpus heterophyllus)* leave template synthesized ZnO nanoparticle with hexagonal wurtzite structure and 15–25 nm particles size ranging exhibited excellent photodegradation efficiency (> 80%, 0.24 g/L, 1 h) against Rose Bengal dye, the main water-pollutant released by the textile industries. Bacteria (*Bacillus licheniformis*) mediated synthesized ZnO nanoflowers, shows a remarkable photocatalytic degradation of methylene blue (MB) dye under UV-irradiation for 60 min to achieve 83% with three times efficient recovery of the ZnO nanoflower as reported by Tripathi et al. [131].

Zheng et al. [89] synthesized ZnONP using the *Corymbia citriodora* leaf extract as a bio-reductant for MB degradation in comparison to the same nanoparticle prepared by hydrothermal method. The bioinspired ZnONP (20 mg) shows 83.45% degradation while the conventionally synthesized ZnONP shows only 59.47 degradation efficiency in 90 min under the visible light irradiation. Prasad et al. [102] synthesized ZnO nanoparticles using lemon juice as a capping agent and ethylene glycol as a solvent. They synthesized the nanoparticle in average 49.16 nm size and hexagonal wurtzite morphology. The ZnO nanogranules (100 mg) was tested to degrade three different dye solutions of methylene blue (MB) (31.98 mg/L), congo red (CR) (67.16 mg/L) and Rhodamine B (Rh-B) (47.90 mg/L) under UV light irradiation; 91.17% of the MB solution was degraded in 70 min, 90% photocatalytic degradation efficiency was achieved for CR solution within 35 min and the degradation of Rh-B is almost complete after 50 min by removing of 98% of the dye molecules from the initial solution. Increase in catalyst load enabled to achieve complete degradation of MB and Rh-B while the catalyst amount was optimized for CR degradation. Photocatalysts such as titanium dioxide (TiO_2) and zinc oxide (ZnO) are semiconductors that able to absorb the energy from light and subsequently excite their electrons from the valence band to conduction band. Zinc oxide is one of the most important functional oxides that has been conventionally applied as photocatalyst owing to its direct band gap, large excitation binding energy and good carrier mobility. Applied zinc oxide nanoparticles in the heterogeneous photocatalytic reaction achieved nearly 95% of congo red dye removal. Besides, successfully embedded zinc oxide into polyvinylidene fluoride (PVDF) microfiltration membrane and improved the hydrophilicity of the membrane. Nevertheless, the distinct band gap energy of zinc oxide (3.2 eV) has restricted the utilization of visible light for the photocatalytic reaction [194]. Maximum degradation (up to 90%) photocatalytic degradation of 2, 4-dichlorophenol is also achieved with the coupled catalyst Zn_2Zr (ZnO and ZrO_2 in 2:1 ratio) at pH 5 for 75 mg/L phenol and 30 mg catalyst load [195].

Micrococcus lylae, Micrococcus aloeverae, Cellulosimicrobium sp. mediated synthesis of TiO_2 nanoparticles in 14–17 nm range particle size and spherical shape was tested for photocatalytic activity of MO, which confirmed that TiO_2 obtained from microbial synthesis using individual bacterial strains show a comparable degradation with the commercial ones ~ 99% degradation of MO in 195, 180, 105 min of the samples respectively under UV irradiation. Similarly, sorghum root extract mediated synthesis of TiO_2 nanoparticles shows 99.7% degradation efficiency in the same condition. The stability and reusability of the photocatalyst TiO_2 is checked, approximately 98% of MO dye solution degradation achieved even after four consecutive runs using the root extracted sample as reported by Fulekar et al. [133].

Green synthesized TiO_2 using soluble starch as the template and titanium (IV) tetraisopropoxide as a metal ion source was carryout to degrade MB under sunlight, stability and reusability of the nanoparticles was checked ten times, after 10 cycles, the degradation efficiency of MB reduced only about 13.3% to 86.7%. Therefore, the study showed that the photocatalytic activity of TiO_2NPs has a good repeatability. Recycled TiO_2NPs for ten times and freshly synthesized TiO_2NPs analyzed by XRD and FESEM and the porosity, morphological stability of the synthesized TiO_2NPs remained same as in anatase phase after ten items of washing as worked by Muniandy et al. [196]. On the other hand, iron (III) oxide, which is abundant in the Earth crust has been applied as photocatalyst owing to its feasibility of photocatalytic process under visible light. From literature, iron (III) oxide has been used as nano-sorbents for heavy metal adsorption and also as a sensitizer for the photocatalytic reactions. Besides, iron (III) oxide has been incorporated with TiO_2 to degrade 4-chlorophenol under visible light [194].

4.5 Proposed reaction mechanism of photocatalysis

When the oxide semiconductor (such as TiO_2, ZnO, ZnS, Fe_2O_3, CdS, WO_3, ZrO_2, SrO_2, CeO_2, etc.) absorbs a photon with energy greater than or equal to the band gap energy, electrons are promoted from the valence band (VB) to the conduction band (CB) to produce electron–hole pairs [197, 198].

$$\text{Photon} + \text{Semiconductor} \rightarrow \text{Semiconductor}\left(e^{-}_{CB} + h^{+}_{VB}\right)$$

Produced electron–hole pairs can either recombine and release heat energy or interact separately with other molecules. The electrons in the conduction band can reduce dissolved oxygen to superoxide radical anion and this radical may form hydrogen peroxide. The electron reduction of hydrogen peroxide produces hydroxyl radical [80].

$$e^{-} + O_{2(ads)} \rightarrow {}^{\cdot}O^{-}_{2(ads)}$$

$${}^{\cdot}O^{-}_{2} + 2H^{+} + 2e^{-} \rightarrow H_2O_2$$

$$H_2O_2 + H^{+} + e^{-} \rightarrow OH^{\cdot} + H_2O$$

The holes in the valence band can oxidize the adsorbed water or hydroxide ions to produce hydroxyl radicals.

$$h^{+} + H_2O_{ads} \rightarrow {}^{\cdot}OH_{(ads)} + H^{+}$$

$$h^{+} + OH^{-}_{ads} \rightarrow {}^{\cdot}OH_{(ads)}$$

Produced free radicals are able to undergo secondary reactions. Among them, the hydroxyl radicals can be used to degrade organic compounds at or near these surfaces of semiconductor catalyst, and intermediates are formed. These intermediates react with hydroxyl radicals to produce final products.

$${}^{\cdot}OH_{ads} + \text{Organic compounds} \rightarrow \text{Intermediates} \rightarrow \text{Products}$$

The CBe^{-} with molecular oxygen produces superoxide radicals $O^{\bullet-}_{2}$ which ultimately reacts with H^{+} to produce $HO^{\bullet}_{2}$radical species. The photoinduced holes can react with water and the dye molecule (R) to yield hydroxyl radical and $R^{\bullet+}$ radical cations. All these oxygenous radicals ($HO^{\bullet}_{2}$, $O^{\bullet-}_{2}$, $OH^{\bullet}$) are powerful oxidizers capable to degrade the organic compound R^{+} further into non-toxic end products [72, 189]. The schematic of the degradation mechanism is shown in Fig. 9.

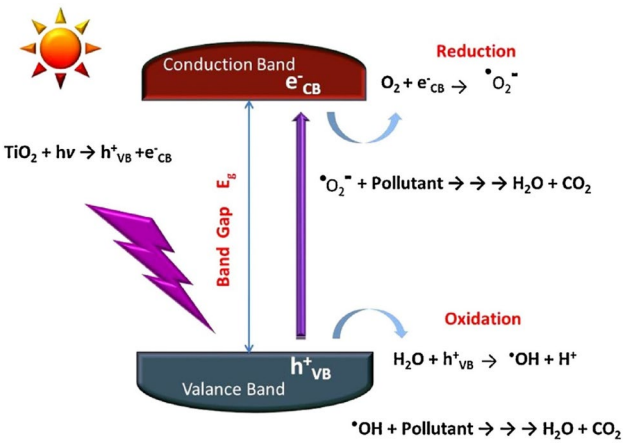

Fig. 9 Mechanism of photocatalysis [196]. © Elsevier, reproduced with permission

Surendra and Roopan [66] fabricated cerium oxide nanoparticles using peel extract of *Moringa oleifera* as reducing/capping agent in a range size of 40–45 nm for the purpose of dye degradation, they have tested the nanoparticles (CeO_2) for the degradation of crystal violet under the UV light by taking 5 mg/L purified CeO_2NPs to the 10 mg/L of crystal violet solution and they have achieved a degradation efficiency of 97.5% exactly in 60 min. Osuntokun et al. [104] work reveals that SnO_2 synthesized nanoparticle via an environmentally friendly route could be utilized in the degradation of toxic organic dyes such as MB. They have prepared two samples regarding their size annealed in a furnace at 300 and 450 °C to have the size of 3.55–5.8 and 5.28–6.34 nm, respectively. The photocatalytic efficiency of the two nanoparticles was checked. An aqueous solution of MB (1×10^{-4} M) was mixed with 20 mg of SnO_2 nanoparticles, and irradiated with UV light, the result shows 91.89 and 88.23% degradation of MB, respectively after 180 min. The variation could be ascribed to the smaller size of the first sample annealed at smaller temperature. Calcination of the sample at high temperature increases the particle size of the nanoparticles which is the main drawback, but crystallinity is increase as a function of temperature [199]. Table 7 shows some photocatalytic studies conducted using biogenically synthesized metal oxide nanoparticles using plant and microorganism as a capping agent.

Table 7 Selected studies of plant and microorganism mediated metal oxide synthesized NPs for photocatalytic activity

Microorganism/plant	NPs	Removal target	Initial concentration	Dose of NPs	Irradiation time (min)	Radiation source	Removal efficiency (%)	References
Cassia fistula, leave	ZnO	Methylene blue	5 ppm	50 mg	90–120	Sun light, UV light	98.71	[84]
Artocarpus heterophyllus, leave	ZnO	Rose Bengal	0.24 g/L	60 mg	60	UV light	85	[70]
Bacillus licheniformis	ZnO	Methylene blue	0.25 g/L)	100 µm/L	60	UV light	83	[131]
lemon juice	ZnO	Methylene blue	31.98 mg/L	100 mg	70	UV light	91.17	[102]
		Congo red	67.16 mg/L	100 mg	35	UV light	90	[102]
		Rhodamine B	47.90 mg/L	100 mg	50	UV light	98	[102]
Citrus aurantifolia (lemon), *Citrus paradisi*	ZnO	Methylene blue	15 mg/L	15 mg/L	180	UV light	97	[59]
Micrococcus lylae	TiO_2	Methyl Orange	0.02 mmol/L	0.03 g	195	UV light	99	[133]
Cellulosimicrobium sp.	TiO_2	Methyl Orange	0.02 mmo/L	0.03 g	105	UV light	99	[133]
Bacillus Amyloliquefaciens	TiO_2	Reactive Red 31	75 ppm	0.4 g	60	UV light	90.98	[125]
Starch	TiO_2	Methylene blue	6 mg/L	0.1 g	120	Sun light	100	[196]
Moringa oleifera, peel	CeO_2	Crystal violet	10 mg/L	5 mg/L	60	UV light	97.5	[66]
Cauliflower	SnO_2	Methylene blue	1×10^{-4} M	20 mg	180	UV light	91.89	[104]
Azadirachta indica	CeO_2	Rhodamine B	10 ppm	100 mg	120	UV light	96	[200]
Tamarindus indica	TiO_2	Titan Yellow	10 ppm	0.75 g/L	120	UV light	96.04	[152]

5 Conclusion and future prospects

The novel properties of nanomaterials generated from their synthesis routs led to new directions for synthesis in different aspects. Metal oxide nanomaterials can be synthesized using physical, chemical and biological methods, and the biological method is the most promising one due to ecofriendly, cost effected and simple experimentation. The bioinspired synthesized metal oxide nanoparticles have a diverse application in terms of nanomedicine, water and soil treatment, agricultural, energy and mixed consumer products. Due to environmental concerns of using various toxic chemicals for the synthesis of metal oxides, completely new strategies have been built and biosynthesis draws the attentions of many researchers. In most of the cases, the mechanism of fabrication involves the reduction of metal salt into corresponding metal ion followed by the formation of a complex with the most active and abundant chemical present in the biological source. Hence, the calcination of this ultimately leads to the formation of corresponding oxide material. The biosynthesis strategy has several advantages over conventional chemical-based techniques. It requires less toxic chemicals and the experimental technique is simple and environmentally benign. Moreover, the cost of fabricating these materials is still less compared to other techniques. However, reproducibility, scale up production procedures, and the mechanism of the nanoparticle synthesis need to be investigated and elucidated clearly. To date, wide variety of metal oxides with very interesting size and shape have been produced. Biologically synthesized metal oxide nanoparticles such as ZnO, TiO_2, Fe_2O_3, Fe_3O_4, CeO_2, NiO, CuO, and SnO_2 have been employed to decontaminate wastewater, inhibit the growth of bacteria and fungi.

Therefore, the focus should be made more on the greener approach for the synthesis of metal oxide nanoparticles, which would, to some extent, help in limiting toxicity towards the environment. Besides this some studies show that bacteria are among the least sensitive organisms to nanoparticles (CuO and ZnO). It was found that crustaceans, algae and fish were more sensitive to these nanoparticles toxicity. Hence, the release of these nanoparticles into waste streams may pose threat to the non-target organisms in the aquatic system and a consideration must take in this case [166].

Compliance with ethical standards

Conflict of interest On behalf of all authors, the corresponding author states that there is no conflict of interest.

References

1. Das VL, Thomas R, Varghese RT, Soniya EV, Mathew J, Radhakrishnan EK (2014) Extracellular synthesis of silver nanoparticles by the *Bacillus strain* CS 11 isolated from industrialized area. Biotech 4:121–126
2. Rao T, Apparao K, Murthy S, Naidu TM (2016) Applications of zinc oxide nanoparticles as catalyst in dissipation kinetics of S-metolachlor herbicide in different pH waters under direct sun light. Mater Today Proc 3:3799–3804
3. Yu S, Liu J, Yin Y, Shen M (2017) Interactions between engineered nanoparticles and dissolved organic matter: a review on mechanisms and environmental effects. J Environ Sci 63:198–217
4. Pachapur VL, Larios AD, Cledón M, Brar SK, Verma M, Surampalli RY (2016) Behavior and characterization of titanium dioxide and silver nanoparticles in soils. Sci Total Environ 563–564:933–943
5. Dinesh R, Anandaraj M, Srinivasan V, Hamza S (2012) Engineered nanoparticles in the soil and their potential implications to microbial activity. Geoderma 173–174:19–27
6. Puay N, Qiu G, Ting Y (2015) Effect of zinc oxide nanoparticles on biological wastewater treatment in a sequencing batch reactor. J Clean Prod 88:139–145
7. Saif S, Tahir A, Chen Y (2016) Green synthesis of iron nanoparticles and their environmental applications and implications. Nanomaterials 6:1–26
8. Amde M, Liu J, Tan Z, Bekana D (2017) Transformation and bioavailability of metal oxide nanoparticles in aquatic and terrestrial environments. A review. Environ Pollut 230:250–267
9. Seabra AB, Durán N (2015) Nanotoxicology of metal oxide nanoparticles. Metals (Basel) 5:934–975
10. Shanker U, Jassal V, Rani M (2016) Catalytic removal of organic colorants from water using some transition metal oxide nanoparticles synthesized under sunlight. RSC Adv 6:94989–94999
11. Kaur P, Thakur R, Duhan JS, Chaudhury A (2018) Management of wilt disease of chickpea in vivo by silver nanoparticles biosynthesized by rhizospheric microflora of chickpea (*Cicer arietinum*). J Chem Technol Biotechnol 93:3233–3243
12. Ruddaraju LK, Pammi SVN, Sankar GG, Padavala VS, Kolapalli VRM (2019) A review on anti-bacterials to combat resistance: from ancient era of plants and metals to present and future perspectives of green nano technological combinations. Asian J Pharm Sci. https://doi.org/10.1016/j.ajps.2019.03.002
13. Patra JK, Baek K (2014) Green nanobiotechnology: factors affecting synthesis and characterization techniques. J Nanomater 2014:1–12
14. Kumar B, Smita K, Cumbal L, Debut A, Angulo Y (2017) Biofabrication of copper oxide nanoparticles using Andean blackberry (*Rubus glaucus Benth*.) fruit and leaf. J Saudi Chem Soc 21:S475–S480
15. Shah M, Fawcett D, Sharma S, Tripathy SK, Poinern GEJ (2015) Green synthesis of metallic nanoparticles via biological entities. Materials (Basel) 8:7278–7308
16. Yadav M, Kaur P (2018) A review on exploring phytosynthesis of silver and gold nanoparticles using genus *Brassica*. Int J Nanopart 10(3):165
17. Predescu AM, Matei E, Berbecaru AC, Pantilimon C, Drăgan C, Vidu R, Predescu C, Kuncser V (2018) Synthesis and characterization of dextran-coated iron oxide nanoparticles. R Soc Open Sci 5:1–11
18. Machado S, Pacheco JG, Nouws HPA, Albergaria JT, Delerue-Matos C (2015) Characterization of green zero-valent iron nanoparticles produced with tree leaf extracts. Sci Total Environ 533:76–81
19. Peng Y, Tsai Y, Hsiung C, Lin Y, Shih Y (2017) Influence of water chemistry on the environmental behaviors of commercial ZnO nanoparticles in various water and wastewater samples. J Hazard Mater 322:348–356
20. Ahmed B, Khan MS, Saquib Q, Al-Shaeri M, Musarrat J (2018) Interplay between engineered nanomaterials (ENMs) and edible plants: a current perspective. In: Faisal M, Saquid Q, Alatar AA, Al-Khedhairy AA (eds) Phytotoxicity of nanoparticles. Springer, Riyadh, pp 63–102
21. Ahmed B, Shahida M, Khan MS, Musarrat J (2018) Chromosomal aberrations, cell suppression and oxidative stress generation induced by metal oxide nanoparticles (MONPs) in onion (*Allium cepa*) bulb. Metallomics 10:1315–1327
22. Ahmed B, Dwivedi S, Abdin MZ, Azam A, Al-Shaeri M, Khan MS, Saquib Q, Al-Khedhairy AA, Musarrat J (2017) Mitochondrial and chromosomal damage induced by oxidative stress in Zn^{2+} ions, ZnO-Bulk and ZnO-NPs treated *Allium cepa* roots. Sci Rep 7:1–14
23. Ahmed B, Khan MS, Musarrat J (2018) Toxicity assessment of metal oxide nano-pollutants on tomato (*Solanum lycopersicon*): a study on growth dynamics and plant cell death. Environ Pollut 240:802–816
24. Rashid MI, Shahzad T, Shahid M, Ismail IMI, Shah GM, Almeelbi T (2017) Zinc oxide nanoparticles affect carbon and nitrogen mineralization of *Phoenix dactylifera* leaf litter in a sandy soil. J Hazard Mater 324:298–305
25. Jafarirad S, Mehrabi M, Divband B, Kosari-nasab M (2016) Biofabrication of zinc oxide nanoparticles using fruit extract of Rosa canina and their toxic potential against bacteria: a mechanistic approach. Mater Sci Eng C 59:296–302
26. Rajeshkumar S (2016) Synthesis of silver nanoparticles using fresh bark of *Pongamia pinnata* and characterization of its antibacterial activity against gram positive and gram negative pathogens. Resour Technol 2:30–35
27. Padalia H, Moteriya P, Chanda S (2015) Green synthesis of silver nanoparticles from marigold flower and its synergistic antimicrobial potential. Arab J Chem 8:732–741
28. Sundrarajan M, Ambika S, Bharathi K (2015) Plant-extract mediated synthesis of ZnO nanoparticles using *Pongamia pinnata* and their activity against pathogenic bacteria. Adv Powder Technol 26:1294–1299
29. Yadav KV, Fulekar MH (2018) Biogenic synthesis of maghemite nanoparticles (γ-Fe_2O_3) using *Tridax* leaf extract and its application for removal of fly ash heavy metals (Pb, Cd). Mater Today 5:20704–20710
30. Raghavendra M, Yatish KV, Lalithamba HS (2017) Plant-mediated green synthesis of ZnO nanoparticles using *Garcinia gummi-gutta* seed extract: photoluminescence, screening of their catalytic activity in antioxidant, formylation and biodiesel production. Eur Phys J Plus 132:1–12
31. Karthik S, Siva P, Balu KS, Suriyaprabha R, Rajendran V, Maaza M (2017) *Acalypha indica*—mediated green synthesis of ZnO nanostructures under differential thermal treatment: effect on textile coating, hydrophobicity, UV resistance, and antibacterial activity. Adv Powder Technol 28:3184–3194
32. Swain AK (2016) Review on green synthesis of silver nanoparticles by physical, chemical and biological methods. Int J Sci Eng Res 7:551–554
33. Ismail RA, Ali AK, Ismail MM, Hassoon KI (2011) Preparation and characterization of colloidal ZnO nanoparticles using nanosecond laser ablation in water. Appl Nanosci 1:45–49
34. Carneiro JO, Azevedo S, Fernandes F, Freitas E (2014) Synthesis of iron-doped TiO_2 nanoparticles by ball-milling process: the influence of process parameters on the structural, optical, magnetic, and photocatalytic properties. J Mater Sci 49:7476–7488

35. Kulkarni SK (ed) (2015) Synthesis of nanomaterials—II (Chemical methods). In: Nanotechnology: principles and practices, 3rd edn. Springer, Pune, pp 77–109. https://doi.org/10.1007/978-3-319-09171-6
36. Segovia M, Sotomayor C, Gonzalez G, Benavente E (2012) Zinc oxide nanostructures by solvothermal. Mol Cryst Liq Cryst 555:40–50
37. Samat NA, Nor RM (2013) Sol–gel synthesis of zinc oxide nanoparticles using *Citrus aurantifolia* extracts. Ceram Int 39:S545–S548
38. Jagadhesan S, Senthilkumar N, Senthilnathan V, Senthil TS (2018) Sb doped ZnO nanostructures prepared via co-precipitation approach for the enhancement of MB dye degradation Sb doped ZnO nanostructures prepared via co-precipitation approach for the enhancement of MB dye degradation. Mater Res Express 5:1–8
39. Stankic S, Suman S, Haque F, Vidic J (2016) Pure and multi metal oxide nanoparticles: synthesis, antibacterial and cytotoxic properties. J Nanobiotechnol 14:1–20
40. Hussain I, Singh NB, Singh A, Singh H, Singh SC (2016) Green synthesis of nanoparticles and its potential application Green synthesis of nanoparticles and its potential application. Biotechnol Lett 38:545–560
41. Thakkar KN, Mhatre SS, Parikh RY (2010) Biological synthesis of metallic nanoparticles. Nanomed Nanotechnol Biol Med 6:257–262
42. Akhtar MS, Panwar J, Yun Y (2013) Biogenic synthesis of metallic nanoparticles by plant extracts. Sustain Chem Eng 1:591–602
43. Kaur P, Thakur R, Chaudhury A (2016) Biogenesis of copper nanoparticles using peel extract of *Punica granatum* and their antimicrobial activity against opportunistic pathogens. Green Chem Lett Rev 9:33–38
44. Jeevanandam J, Chan YS, Danquah MK (2016) Biosynthesis of metal and metal oxide nanoparticles. ChemBioEng Rev 3:55–67
45. Silveira C, Shimabuku QL, Silva MF, Bergamasco R (2017) Iron-oxide nanoparticles by green synthesis method using *Moringa oleifera* leaf extract for fluoride removal. Environ Technol 33:2926–2936
46. Ahmed B, Hashmi A, Khan MS, Musarrat J (2018) ROS mediated destruction of cell membrane, growth and biofilms of human bacterial pathogens by stable metallic AgNPs functionalized from bell pepper extract and quercetin. Adv Powder Technol 29:1601–1616
47. Mittat AK, Chisti Y, Banerjee UC (2013) Synthesis of metallic nanoparticles using plant extracts. Biotechnol Adv 31:346–356
48. Rufus A, Sreeju N, Vilas V, Philip D (2017) Biosynthesis of hematite (α-Fe_2O_3) nanostructures: size effects on applications in thermal conductivity, catalysis, and antibacterial activity. J Mol Liq 242:537–549
49. Sundrarajan M, Bama K, Bhavani M, Jegatheeswaran S, Ambika S, Sangili A, Nithya P, Sumathi R (2017) Obtaining titanium dioxide nanoparticles with spherical shape and antimicrobial properties using *M. citrifolia* leaves extract by hydrothermal method. J Photochem Photobiol B Biol 171:117–124
50. Kalyania RL, Pammi SVN, Kumar PPNV, Padavala VS, Murthy KVR (2019) Antibiotic potentiation and anti-cancer competence through bio-mediated ZnO nanoparticles. Mater Sci Eng C 103:109756
51. Nasrollahzadeh M, Sajadi SM (2015) Synthesis and characterization of titanium dioxide nanoparticles using *Euphorbia heteradena Jaub* root extract and evaluation of their stability. Ceram Int 41:14435–14439
52. Madan HR, Sharma SC, Udayabhanu SD, Vidya YS, Nagabhushana H, Rajanaik H, Anantharaju KS, Prashantha SC, Maiya PS (2016) Facile green fabrication of nanostructure ZnO plates, bullets, flower, prismatic tip, closed pine cone: their antibacterial, antioxidant, photoluminescent and photocatalytic properties. Spectrochem Acta Part A Mol Biomol Spectrosc 152:404–416
53. Ali K, Dwivedi S, Azam A, Saquib Q, Al-Said MS, Alkhedhairy AA, Musarrat J (2016) *Aloe vera* extract functionalized zinc oxide nanoparticles as nanoantibiotics against multi-drug resistant clinical bacterial isolates. J Colloid Interface Sci 472:145–156
54. Sharma D, Sabela MI, Kanchi S, Mdluli PS, Singh G, Stenström TA, Bisetty K (2016) Biosynthesis of ZnO nanoparticles using *Jacaranda mimosifolia* flowers extract: synergistic antibacterial activity and molecular simulated facet specific adsorption studies. J Photochem Photobiol B Biol 162:199–207
55. Momeni SS, Nasrollahzadeh M, Rustaiyan A (2016) Green synthesis of the Cu/ZnO nanoparticles mediated by *Euphorbia prolifera* leaf extract and investigation of their catalytic activity. J Colloid Interface Sci 472:173–179
56. Al-ruqeishi MS, Mohiuddin T, Al-saadi LK (2016) Green synthesis of iron oxide nanorods from *deciduous Omani* mango tree leaves for heavy oil viscosity treatment. Arab J Chem 30:1–7. https://doi.org/10.1016/j.arabjc.2016.04.003
57. Kashale AA, Gattu KP, Ghule K, Ingole VH, Dhanayat S, Sharma R, Chang J, Ghule AV (2016) Biomediated green synthesis of TiO_2 nanoparticles for lithium ion battery application. Compos Part B 99:297–304
58. Kumar B, Smita K, Cumbal L, Debut A (2014) Green approach for fabrication and applications of zinc oxide nanoparticles. Bioinorg Chem Appl 2014:1–7
59. Nava OJ, Soto-Robles CA, Gomez-Gutierrez CM, Vilchis-Nestor AR, Castro-Beltran A, Olivas A, Luque PA (2017) Fruit peel extract mediated green synthesis of zinc oxide nanoparticles. J Mol Struct 1147:1–6
60. Bhuyan T, Mishra K, Khanuja M, Prasad R, Varma A (2015) Biosynthesis of zinc oxide nanoparticles from *Azadirachta indica* for antibacterial and photocatalytic applications. Mater Sci Semicond Process 32:55–61
61. Pallela PNVK, Ummey S, Ruddaraju LK, Kollu P, Khan S, Pammi SVN (2019) Antibacterial activity assessment and characterization of green synthesized CuO nano rods using *Asparagus racemosus* roots extract. SN Appl Sci 1:1–6
62. Kumar PPNV, Shameem U, Kollu P (2015) Green synthesis of copper oxide nanoparticles using *Aloe vera* leaf extract and its antibacterial activity against fish bacterial pathogens. BioNanoSci 5:135–139
63. Hariharan D, Srinivasan K, Lc N (2017) Synthesis and characterization of TiO_2 nanoparticles using *Cynodon Dactylon* leaf extract for antibacterial and anticancer (A549 Cell Lines) activity. J Nanomed Res Synth 5:1–5
64. Kumar J, Srivastava P, Ameen S, Akhtar MS, Singh G, Yadava S (2016) *Azadirachta indica* plant-assisted green synthesis of Mn_3O_4 nanoparticles: excellent thermal catalytic performance and chemical sensing behavior. J Colloid Interface Sci 472:220–228
65. Matinise N, Fuku XG, Kaviyarasu K, Mayedwa N, Maaza M (2017) ZnO nanoparticles via *Moringa oleifera* green synthesis: physical properties & mechanism of formation. Appl Surf Sci 406:339–347
66. Surendra TV, Roopan SM (2016) Photocatalytic and antibacterial properties of phytosynthesized CeO_2 NPs using *Moringa oleifera* peel extract. J Photochem Photobiol B Biol 161:122–128
67. Moon S, Salunke B, Alkotaini B, Sathiyamoorthi E, Kim BS (2015) Biological synthesis of manganese dioxide nanoparticles by *Kalopanax pictus* plant extract. IET Nanobiotechnol 9:220–225
68. Prasad AS (2016) Iron oxide nanoparticles synthesized by controlled bio-precipitation using leaf extract of Garlic Vine (*Mansoa alliacea*). Mater Sci Semicond Process 53:79–83

69. Yedurkar S, Maurya C, Mahanwar P (2016) Biosynthesis of zinc oxide nanoparticles using *Ixora Coccinea* leaf extract—a Green approach. Open J Synth Theory Appl 5:1–14
70. Vidya C, Prabha MNC, Raj MALA (2016) Green mediated synthesis of zinc oxide nanoparticles for the photocatalytic degradation of Rose Bengal dye. Environ Nanotechnol Monit Manag 6:134–138
71. Anbuvannan M, Ramesh M, Viruthagiri G, Shanmugam N, Kannadasan N (2015) *Anisochilus carnosus* leaf extract mediated synthesis of zinc oxide nanoparticles for antibacterial and photocatalytic activities. Mater Sci Semicond Process 39:621–628
72. Stan M, Popa A, Toloman D, Dehelean A, Lung I, Katona G (2015) Enhanced photocatalytic degradation properties of zinc oxide nanoparticles synthesized by using plant extracts. Mater Sci Semicond Process 39:23–29
73. Suresh D, Shobharani RM, Nethravathi PC, Kumar MAP, Nagabhushana H, Sharma SC (2015) *Artocarpus gomezianus* aided green synthesis of ZnO nanoparticles: luminescence, photocatalytic and antioxidant properties. Spectrochim Acta Part A Mol Biomol Spectrosc 141:128–134
74. Kumara PPNV, Pammi SVN, Shameem U (2018) A Green approach for the synthesis of iron oxide nanoparticles by using roots of *A. racemosus* and its degradation of dye methyl orange. Int J Pharm Drug Anal 6:22–28
75. Roopan SM, Bharathi A, Prabhakarn A, Rahuman AA, Velayutham K, Rajakumar G, Padmaja RD, Lekshmi M, Madhumitha G (2012) Efficient phyto-synthesis and structural characterization of rutile TiO_2 nanoparticles using *Annona squamosa* peel extract. Spectrochim Acta Part A Mol Biomol Spectrosc 98:86–90
76. Fu L, Fu Z (2015) *Plectranthus amboinicus* leaf extract-assisted biosynthesis of ZnO nanoparticles and their photocatalytic activity. Ceram Int 41:2492–2496
77. Venkateswarlu S, Rao YS, Balaji T, Prathima B, Jyothi NVV (2013) Biogenic synthesis of Fe_3O_4 magnetic nanoparticles using *plantain* peel extract. Mater Lett 100:241–244
78. Vidhu VK, Philip D (2015) Biogenic synthesis of SnO_2 nanoparticles: evaluation of antibacterial and antioxidant activities. Spectrochim Acta Part A Mol Biomol Spectrosc 134:372–379
79. Anbuvannan M, Ramesh M, Viruthagiri G, Shanmugam N, Kannadasan N (2015) Synthesis, characterization and photocatalytic activity of ZnO nanoparticles prepared by biological method. Spectrochim Acta Part A Mol Biomol Spectrosc 143:304–308
80. Geetha MS, Nagabhushana H, Shivananjaiah HN (2016) Green mediated synthesis and characterization of ZnO nanoparticles using *Euphorbia Jatropa* latex as reducing agent. J Sci Adv Mater Devices 1:301–310
81. Chaudhuri SK, Malodia L (2017) Biosynthesis of zinc oxide nanoparticles using leaf extract of *Calotropis gigantea*: characterization and its evaluation on tree seedling growth in nursery stage. Appl Nanosci 7:501–512
82. Sankar R, Manikandan P, Malarvizhi V, Fathima T, Shivashangari KS, Ravikumar V (2014) Green synthesis of colloidal copper oxide nanoparticles using *Carica papaya* and its application in photocatalytic dye degradation. Spectrochim Acta Part A Mol Biomol Spectrosc 121:746–750
83. Diallo A, Manikandan E, Rajendran V, Maaza M (2016) Physical and enhanced photocatalytic properties of green synthesized SnO_2 nanoparticles via Aspalathus linearis. J Alloys Compd 681:561–570
84. Suresh D, Nethravathi PC, Udayabhanu A, Rajanaika H, Nagabhushana H, Sharma SC (2015) Green synthesis of multifunctional zinc oxide (ZnO) nanoparticles using *Cassia fistula* plant extract and their photodegradative, antioxidant and antibacterial activities. Mater Sci Semicond Process 31:446–454
85. Thovhogi N, Park E, Manikandan E, Maaza M, Gurib-Fakim A (2016) Physical properties of CdO nanoparticles synthesized by green chemistry via *Hibiscus Sabdariffa* flower extract. J Alloys Compd 655:314–320
86. Thema FT, Manikandan E, Dhlamini MS, Maaza M (2015) Green synthesis of ZnO nanoparticles via *Agathosma betulina* natural extract. Mater Lett 161:124–127
87. Thema FT, Manikandan E, Gurib-fakim A, Maaza M (2016) Single phase Bunsenite NiO nanoparticles green synthesis by *Agathosma betulina* natural extract. J Alloys Compd 657:655–661
88. Nagajyothi PC, An TNM, Sreekanth TVM, Lee J, Lee DJ, Lee KD (2013) Green route biosynthesis: characterization and catalytic activity of ZnO nanoparticles. Mater Lett 108:160–163
89. Zheng Y, Fu L, Han F, Wang A, Cai W, Yu J, Yang J, Peng F (2015) Green biosynthesis and characterization of zinc oxide nanoparticles using *Corymbia citriodora* leaf extract and their photocatalytic activity. Green Chem Lett Rev 8:59–63
90. Balaji S, Kumar MB (2017) Facile green synthesis of zinc oxide nanoparticles by *Eucalyptus globulus* and their photocatalytic and antioxidant activity. Adv Powder Technol 28:785–797
91. Dhanemozhi AC, Rajeswari V, Sathyajothi S (2017) Green synthesis of zinc oxide nanoparticle using green tea leaf extract for supercapacitor application. Mater Today Proc 4:660–667
92. Vanathi P, Rajiv P, Narendhran S, Rajeshwari S, Rahman PKSM, Venckatesh R (2014) Biosynthesis and characterization of phyto mediated zinc oxide nanoparticles: a green chemistry approach. Mater Lett 134:13–15
93. Ahmmad B, Leonard K, Islam S, Kurawaki J, Muruganandham M, Ohkubo T, Kuroda Y (2013) Photocatalytic activity Green synthesis of mesoporous hematite (α-Fe_2O_3) nanoparticles and their photocatalytic activity. Adv Powder Technol 24:160–167
94. Roopan MS, Kumar SHS, Madhumitha G, Suthindhiran K (2015) Biogenic-production of SnO_2 nanoparticles and its cytotoxic effect against hepatocellular carcinoma cell line (HepG2). Appl Biochem Biotechnol 175:1567–1575
95. Qu J, Yuan X, Wang X, Shao P (2011) Zinc accumulation and synthesis of ZnO nanoparticles using *Physalis alkekengi* L. Environ Pollut 159:1783–1788
96. Suman T, Ravindranath R, Elumalai D, Kaleena PK, Ramkumar R, Perumal P, Aranganathan L, Chitrarasu PS (2015) Larvicidal activity of titanium dioxide nanoparticles synthesized using *Morinda citrifolia* root extract against *nopheles stephensi, Aedes Aaegypti* and *Culex quinquefasciatu*s and its other effect on non-target fish. Asian Pacific J Trop Dis 5(3):224–230
97. Santhoshkumar T, Rahuman AA, Jayaseelan C, Rajakumar G, Marimuthu S, Kirthi AV, Velayutham K, Thomas J, Venkatesan J, Kim S (2014) Green synthesis of titanium dioxide nanoparticles using *Psidium guajava* extract and its antibacterial and antioxidant properties. Asian Pac J Trop Med 7:968–976
98. Sutradhar P, Saha M (2016) Green synthesis of zinc oxide nanoparticles using tomato (*Lycopersicon esculentum*) extract and its photovoltaic application. J Exp Nanosci 11:314–327
99. Ijaz F, Shahid S, Khan SA, Ahmad W, Zaman S (2017) Green synthesis of copper oxide nanoparticles using *Abutilon indicum* leaf extract: antimicrobial, antioxidant and photocatalytic dye degradation activities. Trop J Pharm Res 16:743–753
100. Fowsiya J, Madhumitha G, Al-dhabi NA, Valan MA (2016) Photocatalytic degradation of Congo red using *Carissa edulis* extract capped zinc oxide nanoparticles. J Photochem Photobiol B Biol 162:395–401
101. Fazlzadeh M, Khosravi R, Zarei A (2017) Green synthesis of zinc oxide nanoparticles using *Peganum harmala* seed extract, and loaded on *Peganum harmala* seed powdered activated carbon as new adsorbent for removal of Cr(VI) from aqueous solution. Ecol Eng 103:180–190

102. Prasad AR, Ammal PR, Joseph A (2018) Effective photocatalytic removal of different dye stuffs using green synthesized zinc oxide nanogranules. Mater Res Bull 102:116–121
103. Malleshappa J, Nagabhushana H, Sharma SC, Vidya YS, Anantharaju KS, Prashantha SC, Prasad BD, Naika HR, Lingaraju K, Surendra BS (2015) *Leucas aspera* mediated multifunctional CeO_2 nanoparticles: structural, photoluminescent, photocatalytic and antibacterial properties. Spectrochem Acta Part A Mol Biomol Biomol Spectrosc 149:452–462
104. Osuntokun J, Onwudiwe DC, Ebenso EE (2017) Biosynthesis and photocatalytic properties of SnO_2 nanoparticles prepared using aqueous extract of cauliflower. J Clust Sci 28:1883–1896
105. Kumar PN, Sakthivel K, Balasubramanian V (2017) Microwave assisted biosynthesis of rice shaped ZnO nanoparticles using *Amorphophallus konjac* tuber extract and its application in dye sensitized solar cells. Mater Sci 35:111–119
106. Haritha E, Roopan SM, Madhavi G, Elango G, Al-Dhabi NA, Arasu MA (2016) Green chemical approach towards the synthesis of SnO_2NPs in argument with photocatalytic degradation of diazo dye and its kinetic studies. J Photochem Photobiol B Biol 162:441–447
107. Elango G, Kumaran SM, Kumar SS, Muthuraja S, Roopan SM (2015) Green synthesis of SnO_2 nanoparticles and its photocatalytic activity of phenolsulfonphthalein dye. Spectrochim Acta Part A Mol Biomol Spectrosc 145:176–180
108. Goutam SP, Saxena G, Singh V, Yadav AK, Bharagava RN, Thapa KB (2018) Green synthesis of TiO_2 nanoparticles using leaf extract of *Jatropha curcas* L. for photocatalytic degradation of tannery wastewater. Chem Eng J 336:386–396
109. Saleem S, Ahmed B, Khan MS, Al-Shaeri M, Musarrat J (2017) Inhibition of growth and biofilm formation of clinical bacterial isolates by NiO nanoparticles synthesized from *Eucalyptus globulus* plants. Microb Pathog 111:375–387
110. Ali K, Ahmed B, Saghir M, Musarrat J (2018) Differential surface contact killing of pristine and low EPS *Pseudomonas aeruginosa* with *Aloe vera* capped hematite (α-Fe_2O_3) nanoparticles. J Photochem Photobiol B Biol 188:146–158
111. Velusamy P, Kumar GV, Jeyanthi V, Das J, Pachaiappan R (2016) Bio-inspired green nanoparticles: synthesis, mechanism, and antibacterial application. Toxicol Res 32:95–102
112. Deyab M, Elkatony T, Ward F (2016) Qualitative and quantitative analysis of phytochemical studies on brown seaweed, *Dictyota dichotoma*. Int J Eng Dev Res 4:674–678
113. El-din SMM, El-ahwany AMD (2016) Bioactivity and phytochemical constituents of marine red seaweeds (*Jania rubens, Corallina mediterranea* and *Pterocladia capillacea*). Integr Med Res 10:471–484
114. Murugan K, Roni M, Panneerselvam C, Aziz AT, Suresh U, Rajaganesh R, Aruliah R, Mahyoub JA, Trivedi S, Rehman H, Al-Aoh HAN, Kumar S, Higuchi A, Vaseeharan B, Wei H, Senthil-Nathan S, Canale A, Benelli G (2018) *Sargassum wightii* -synthesized ZnO nanoparticles reduce the fitness and reproduction of the malaria vector *Anopheles stephensi* and cotton bollworm *Helicoverpa armigera*. Physiol Mol Plant Pathol 101:202–213
115. Ishwarya R, Vaseeharan B, Kalyani S, Banumathi B, Govindarajan M, Alharbi NS, Kadaikunnan S, Al-anbr MN, Khaled JM, Benelli G (2018) Facile green synthesis of zinc oxide nanoparticles using *Ulva lactuca* seaweed extract and evaluation of their photocatalytic, antibio film and insecticidal activity. J Photochem Photobiol B Biol 178:249–258
116. Yew YP, Shameli K, Miyake M, Kuwano N, Khairudin NBBA, Mohamad ESB, Lee KX (2016) Green synthesis of magnetite (Fe_3O_4) nanoparticles using seaweed (*Kappaphycus alvarezii*) extract. Nanoscale Res Lett 11:1–7
117. Azizi S, Ahmad MB, Namvar F, Mohamad R (2014) Green biosynthesis and characterization of zinc oxide nanoparticles using brown marine macroalga *Sargassum muticum* aqueous extract. Mater Lett 116:275–277
118. Mahdavi M, Namvar F, Ahmad MB, Mohamad R (2013) Green biosynthesis and characterization of magnetic iron oxide (Fe_3O_4) nanoparticles using seaweed (*Sargassum muticum*) aqueous extract. Molecules 18:5954–5964
119. Abboud Y, Saffaj T, Chagraoui A, Bouari AE, Brouzi K, Tanane O, Ihssane B (2014) Biosynthesis, characterization and antimicrobial activity of copper oxide nanoparticles (CuONPs) produced using brown alga extract (*Bifurcaria bifurcata*). Appl Nanosci 4:571–576
120. Rao MD, Gautam P (2016) Synthesis and characterization of ZnO nanoflowers using *Chlamydomonas reinhardtii*: a Green approach. Environ Prog Sustain Energy 35:1020–1026
121. Priyadharshini RI, Prasannaraj G, Geetha N, Venkatachalam P (2014) Microwave-mediated extracellular synthesis of metallic silver and zinc oxide nanoparticles using macro-algae (*Gracilaria edulis*) extracts and its anticancer activity against human PC3 cell lines. Appl Biochem Biotechnol 174:2777–2790
122. Moghaddam AB, Namvar F, Moniri M, Tahir PM, Azizi S, Mohamad R (2015) Nanoparticles biosynthesized by fungi and yeast: a review of their preparation, properties, and medical applications. Molecules 20:16540–16565
123. Ghosh PR, Fawcett D, Sharma SB, Poinern GEJ (2017) Production of high-value nanoparticles via horticultural food waste. Materials (Basel) 10:1–19
124. Kirthi AV, Rahuman AA, Rajakumar G, Marimuthu S, Santhoshkumar T, Jayaseelan C, Elango G, Zahir AA, Kamaraj C, Bagavan A (2011) Biosynthesis of titanium dioxide nanoparticles using bacterium *Bacillus subtilis*. Mater Lett 65:2745–2747
125. Khan R, Fulekar MH (2016) Biosynthesis of titanium dioxide nanoparticles using *Bacillus amyloliquefaciens* culture and enhancement of its photocatalytic activity for the degradation of a sulfonated textile dye Reactive Red 31. J Colloid Interface Sci 475:184–191
126. Órdenes-aenishanslins NA, Saona LA, Durán-toro VM, Monrás JP, Bravo DM, Pérez-Donoso JM (2014) Use of titanium dioxide nanoparticles biosynthesized by *Bacillus mycoides* in quantum dot sensitized solar cells. Microb Cell Fact 13:1–10
127. Jayaseelan C, Rahuman AA, Kirthi AV, Marimuthu S, Santhoshkumar T, Bagavan A, Gaurav K, Karthik L, Rao KVB (2012) Novel microbial route to synthesize ZnO nanoparticles using *Aeromonas hydrophila* and their activity against pathogenic bacteria and fungi. Spectrochim Acta Part A Mol Biomol Spectrosc 90:78–84
128. Jayaseelan C, Rahuman AA, Roopan SM, Kirthi AV, Venkatesan J, Kim S, Iyappan M, Siva C (2013) Biological approach to synthesize TiO_2 nanoparticles using *Aeromonas hydrophila* and its antibacterial activity. Spectrochim Acta Part A Mol Biomol Spectrosc 107:82–89
129. Kundu D, Hazra C, Chatterjee A, Chaudhari A, Mishra S (2014) Extracellular biosynthesis of zinc oxide nanoparticles using *Rhodococcus pyridinivorans NT2*: multifunctional textile finishing, biosafety evaluation and in vitro drug delivery in colon carcinoma. J Photochem Photobiol B Biol 140:194–204
130. Dhandapani P, Maruthamuthu S, Rajagopal G (2012) Bio-mediated synthesis of TiO_2 nanoparticles and its photocatalytic effect on aquatic biofilm. J Photochem Photobiol B Biol 110:43–49
131. Tripathi RM, Bhadwal AS, Gupta RK, Singh P, Shrivastav A, Shrivastav BR (2014) ZnO nanoflowers: novel biogenic synthesis and enhanced photocatalytic activity. J Photochem Photobiol B Biol 141:288–295
132. Sathyavathi S, Manjula A, Rajendhran J, Gunasekaran P (2014) Extracellular synthesis and characterization of nickel oxide nanoparticles from *Microbacterium sp. MRS-1* towards

bioremediation of nickel electroplating industrial effluent. Bioresour Technol 165:270–273
133. Fulekar J, Dutta DP, Pathak B, Fulekar MH (2017) Novel microbial and root mediated green synthesis of TiO_2 nanoparticles and its application in wastewater remediation. J Chem Technol Biotechnol 93:736–743
134. Salaheldin TA, Husseiny SM, Al-enizi AM, Elzatahry A, Cowley AH (2016) Evaluation of the cytotoxic behavior of fungal extracellular synthesized ag nanoparticles using confocal laser scanning microscope. Int J Mol Sci 17:2–11
135. Khandel P, Shahi SK (2018) Mycogenic nanoparticles and their bio-prospective applications: current status and future challenges. J Nanostruct Chem 8:369–391
136. Rajakumar G, Rahuman AA, Roopan SM, Khanna VG, Elango G, Kamaraj C, Zahir AA, Velayutham K (2012) Fungus-mediated biosynthesis and characterization of TiO_2 nanoparticles and their activity against pathogenic bacteria. Spectrochim Acta Part A Mol Biomol Spectrosc 91:23–29
137. Raliya R, Biswas P, Tarafdar JC (2015) TiO_2 nanoparticle biosynthesis and its physiological effect on mung bean (*Vigna radiata* L.). Biotechnol Rep 5:22–26
138. Silva LP, Bonatto CC, Polez VLP (2016) Green synthesis of metal nanoparticles by fungi: current trends and challenges. In: Prasad R (ed) Advances and applications through fungal nanobiotechnology. Springer, Galway, pp 71–90
139. Raliya R, Tarafdar J (2013) ZnO nanoparticle biosynthesis and its effect on phosphorous-mobilizing enzyme secretion and gum contents in clusterbean (*Cyamopsis tetragonoloba* L.). Agric Res 2:48–57
140. Ibrahem EJ, Thalij KM, Saleh MK, Badawy AS (2017) Biosynthesis of zinc oxide nanoparticles and assay of antibacterial activity. Am J Biochem Biotechnol 13:63–69
141. Chauhan R, Reddy A, Abraham J (2015) Biosynthesis of silver and zinc oxide nanoparticles using *Pichia fermentans JA2* and their antimicrobial property. Appl Nanosci 5:63–71
142. Gopinath K, Karthika V, Sundaravadivelan C, Gowri S, Arumugam A (2015) Mycogenesis of cerium oxide nanoparticles using *Aspergillus niger* culture filtrate and their applications for antibacterial and larvicidal activities. J Nanostruct Chem 5:295–303
143. Atalay FE, Asma D, Kaya H, Bingol A, Yaya P (2016) Synthesis of NiO nanostructures using *Cladosporium cladosporioides* fungi for energy storage applications. Nanomater Nanotechnol 6:1–6
144. Salvadori MR, Ando RA, Nascimento CAO, Corrêa B (2015) Extra and intracellular synthesis of nickel oxide nanoparticles mediated by dead fungal biomass. J pone 10:1–15
145. Khan SA, Ahmad A (2013) Fungus mediated synthesis of biomedically important cerium oxide nanoparticles. Mater Res Bull 48:4134–4138
146. Lin P, Lin S, Wang PC, Sridhar R (2014) Techniques for physicochemical characterization of nanomaterials. Biotechnol Adv 32:711–726
147. Suresh J, Pradheesh G, Alexramani V, Sundrarajan M, Hong SI (2018) Green synthesis and characterization of zinc oxide nanoparticle using insulin plant (*Costus pictus D*. Don) and investigation of its antimicrobial as well as anticancer activities. Adv Nat Sci Nanosci Nanotechnol 9:1–9
148. Vijayakumar S, Krishnakumar C, Arulmozhi P, Mahadevan S, Parameswari N (2018) Biosynthesis, characterization and antimicrobial activities of zinc oxide nanoparticles from leaf extract of *Glycosmis pentaphylla* (Retz.) DC. Microb Pthogenes 116:44–48
149. Fardood ST, Ramazani A, Moradi S, Asiabi PA (2017) Green synthesis of zinc oxide nanoparticles using arabic gum and photocatalytic degradation of direct blue 129 dye under visible light. J Mater Sci Mater Electron 28:13596–13601
150. Nagajyothi PC, Pandurangan M, Kim DH, Sreekanth TVM, Shim J (2016) Green synthesis of iron oxide nanoparticles and their catalytic and in vitro anticancer activities. J Clust Sci 28:245–257
151. Malarkodi C, Malik V, Uma S (2018) Synthesis of Fe_2O_3 using *Emblica officinalis* extract and its photocatalytic efficiency. Mater Sci An Indian J 16:1–10
152. Hiremath S, Raj MALA, Prabha MNC, Vidya C (2018) Tamarindus indica mediated biosynthesis of nano TiO_2 and its application in photocatalytic degradation of Titan yellow. J Environ Chem Eng 6:7338–7346
153. Pavithra NS, Lingaraju K, Raghu GK, Nagaraju G (2017) *Citrus maxima* (Pomelo) juice mediated eco-friendly synthesis of ZnO nanoparticles: applications to photocatalytic, electrochemical sensor and antibacterial activities. Spectrochim Acta Part A Mol Biomol Spectrosc 185:11–19
154. Azizi S, Shahri MM, Mohamad R (2017) Green synthesis of zinc oxide nanoparticles for enhanced adsorption of lead ions from aqueous solutions: equilibrium, kinetic and thermodynamic studies. Molecules 22:1–14
155. Ramesh M, Anbuvannan M, Viruthagiri G (2015) Green synthesis of ZnO nanoparticles using S*olanum nigrum* leaf extract and their antibacterial activity. Spectrochim Acta Part A Mol Biomol Spectrosc 136:864–870
156. Venkateswarlu S, Kumar BN, Prasad CH, Venkateswarlu P, Jyothi NVV (2014) Bio-inspired green synthesis of Fe_3O_4 spherical magnetic nanoparticles using *Syzygium cumini* seed extract. Phys B 449:67–71
157. Khalil AT, Ovais M, Ullah I, Ali M, Shinwari KZ, Maaza M (2017) Biosynthesis of iron oxide (Fe_2O_3) nanoparticles via aqueous extracts of *Sageretia thea* (Osbeck.) and their pharmacognostic properties. Green Chem Lett Rev 10:186–201
158. Das AK, Marwal A, Divya S, Pareek V (2015) One-step green synthesis and characterization of plant protein-coated mercuric oxide (HgO) nanoparticles: antimicrobial studies. Int Nano Lett 5:125–132
159. Chandrasekhar M, Nagabhushana H, Sudheerkumar KH, Dhananjaya N, Sharma SC, Kavyashree D, Shivakumara C, Nagabhushana BM (2014) Comparison of structural and luminescence properties of Dy_2O_3 nanopowders synthesized by co-precipitation and green combustion routes. Mater Res Bull 55:237–245
160. Diallo A, Beye AC, Doyle TB, Park E, Maaza M (2015) Green synthesis of Co_3O_4 nanoparticles via *Aspalathus linearis*: physical properties. Green Chem Lett Rev 8:30–36
161. Lin S, Huang R, Cheng Y, Liu J, Lau BLT, Wiesner MR (2012) Silver nanoparticle-alginate composite beads for point-of-use drinking water disinfection. Water Res 47:3959–3965
162. Kumar T, Majid MAA, Onichandran S, Jaturas N, Andiappan H, Salibay CC, Tabo HAL, Tabo N, Dungca JZ, Tangpong J, Phiriyasamith S, Yuttayong B, Polseela R, Do BN, Sawangjaroen N, Tan T, Lim YAL, Nissapatorn V (2016) Presence of *cryptosporidium parvum* and *giardia lamblia* in water samples from Southeast Asia: towards an integrated water detection system. Infect Dis Poverty 5:1–12
163. Özdemir K (2014) Characterization of natural organic matter in conventional water treatment processes and evaluation of THM formation with chlorine. Sci World J 2014:1–7
164. Zazouli MA, Kalankesh LR (2017) Removal of precursors and disinfection by products (DBPs) by membrane filtration from water; a review. J Environ Heal Sci Eng 15:1–10
165. Getaye M, Hagos S, Alemu Y, Tamene Z, Yadav OP (2017) Removal of malachite green from contaminated water using electro-coagulation technique. J Anal Pharm Res 6:1–5

166. Dimapilis EAS, Hsu C, Mendoza RMO, Lu MC (2018) Zinc oxide nanoparticles for water disinfection. Sustain Environ Res 28:47–56
167. Ibrahim RK, Hayyan M, AlSaadi MA, Hayyan A, Ibrahim S (2016) Environmental application of nanotechnology: air, soil, and water. Environ Sci Pollut Res 23:13754–13788
168. Ma L, Wei Q, Chen Y, Song Q, Sun C, Wang Z, Wu G (2018) Removal of cadmium from aqueous solutions using industrial coal fly ash-nZVI. R Soc Open Sci 5:1–9
169. Srivastava V, Gusain D, Sharma YC (2013) Synthesis, characterization and application of zinc oxide nanoparticles (n-ZnO). Ceram Int 39:9803–9808
170. Ehrampoush MH, Miria M, Salmani MH, Mahvi AH (2015) Cadmium removal from aqueous solution by green synthesis iron oxide nanoparticles with *tangerine* peel extract. J Environ Heal Sci Eng 13:1–7
171. Somu P, Paul S (2018) Casein based biogenic-synthesized zinc oxide nanoparticles simultaneously decontaminate heavy metals, dyes, and pathogenic microbes: a rational strategy for wastewater treatment. J Chem Technol Biotechnol 93:2962–2976
172. Shikha D, Sharma CY (2017) *Calotropis procera* mediated one pot green synthesis of Cupric oxide nanoparticles (CuONPs) for adsorptive removal of Cr(VI) from aqueous solutions. Appl Organometal Chem 31:1–15
173. El-deen SEAS, Zhang F (2016) Immobilisation of TiO_2 nanoparticles on sewage sludge and their adsorption for cadmium removal from aqueous solutions. J Exp Nanosci 11:239–258
174. Wang C, Liu H, Liu Z, Gao Y, Wu B, Xu H (2018) Fe_3O_4 nanoparticle-coated mushroom source biomaterial for Cr(VI) polluted liquid treatment and mechanism research. Roral Soc Open Sci 5:1–14
175. Gnanasangeetha D, Umamageshwari TSR (2017) Green synthesis of zinc oxide nanoparticles for water remediation. Int J ChemTech Res 10:101–107
176. Venkateswarlu S, Yoon M (2015) Rapid removal of cadmium ions using green- synthesized Fe_3O_4 nanoparticles capped with diethyl-4-(4-amino-5-mercapto-4H-1,2,4-triazol-3-yl) phenyl phosphonate. RSC Adv 5:65444–65453
177. Mukherjee D, Ghosh S, Majumdar S, Annapurna K (2016) Green synthesis of α-Fe_2O_3 nanoparticles for arsenic(V) remediation with. Biochem Pharmacol 4:639–650
178. Suriyaraj SP, Selvakumar R (2016) Advances in nanomaterial based approaches for enhanced fluoride and nitrate removal from contaminated water. RSC Adv 6:10565–10583
179. Zeng Y, Xue Y, Liang S, Zhang J (2017) Removal of fluoride from aqueous solution by TiO_2 and TiO_2–SiO_2 nanocomposite. Chem Speciat Bioavailab 29:25–32
180. Chai L, Wang Y, Zhao N, Yang Y, You X (2013) Sulfate-doped Fe_3O_4/Al_2O_3 nanoparticles as a novel adsorbent for fluoride removal from drinking water. Water Res 47:4040–4049
181. Kumari S, Khan S (2017) Defluoridation technology for drinking water and tea by green synthesized Fe_3O_4/Al_2O_3 nanoparticles coated polyurethane foams for rural communities. Sci Rep 7:1–12
182. Suriyaraj SP, Vijayaraghavan T, Biji P, Selvakumar R (2014) Adsorption of fluoride from aqueous solution using different phases of microbially synthesized TiO_2 nanoparticles. J Environ Chem Eng 2:444–454
183. El-Aassar AHM, Said MM, Abdel-Gawad AM, Shawky HA (2013) Using silver nanoparticles coated on activated carbon granules in columns for microbiological pollutants water disinfection in Abu. Aust J Basic Appl Sci 7:422–432
184. Xu Y, Li C, Zhu X, Huang WE, Zhang D (2014) Application of mgnetic nanoparticles in drinking water purifucation. Environ Eng Manag J 13:2023–2029
185. Mostafaii G, Chimehi E, Gilasi H, Iranshahi L (2017) Investigation of zinc oxide nanoparticles effects on removal of total coliform bacteria in activated sludge process effluent of municipal wastewater. J Environ Sci Technol 10:49–55
186. Sharmila G, Muthukumaran C, Santhiya K, Santhiya S, Pradeep RS, Kumar NM, Suriyanarayanan N, Thirumarimurugan M (2018) Biosynthesis, characterization, and antibacterial activity of zinc oxide nanoparticles derived from *Bauhinia tomentosa* leaf extract. J Nanostruct Chem 8:293–299
187. Kaur P, Thakur R, Kumar S, Dilbaghi N (2011) Interaction Of ZnO nanoparticles with food borne pathogens *Escherichia coli* DH5α and *Staphylococcus aureus* 5021 and their bactericidal efficacy. Am Inst Phys 153:153–154
188. Sankar R, Prasath BB, Nandakumar R, Santhanam P, Shivashangari KS, Ravikumar V (2014) Growth inhibition of bloom forming *cyanobacterium Microcystis aeruginosa* by green route fabricated copper oxide nanoparticles. Env Sci Pollut Res 21:1–9
189. Subha PP, Jayaraj MK (2015) Solar photocatalytic degradation of methyl orange dye using TiO_2 nanoparticles synthesised by sol–gel method in neutral medium. J Exp Nanosci 10:1106–1115
190. Lee KM, Lai CW, Ngai KS, Juan JC (2016) Recent developments of zinc oxide based photocatalyst in water treatment technology: a review. Water Res 88:428–448
191. Lijuan J, Yajun W, Changgen F (2012) Application of photocatalytic technology in environmental safety. Proc Eng 45:993–997
192. Chong MN, Jin B (2012) Photocatalytic treatment of high concentration carbamazepine in synthetic hospital wastewater. J Hazard Mater 199–200:135–142
193. Kaur P, Thakur R, Malwal H, Manuja A, Chaudhury A (2018) Biosynthesis of biocompatible and recyclable silver/iron and gold/iron core–shell nanoparticles for water purification technology. Biocatal Agric Biotechnol 14:189–197
194. Tan YH, Goh PS, Ismail AF (2015) Development of photocatalytic coupled zinc in iron oxide nanoparticles via solution combustion for bisphenol—a removal. Int Biodeterior Biodegrad 102:346–352
195. Sherly ED, Vijaya JJ, Selvam NCS, Kennedy LJ (2014) Microwave assisted combustion synthesis of coupled ZnO–ZrO_2 nanoparticles and their role in the photocatalytic degradation of 2,4-dichlorophenol. Ceram Int 40:5681–5691
196. Muniandy SS, Kaus NHM, Jiang Z, Altarawneh M, Lee HL (2017) Green synthesis of mesoporous anatase TiO_2 nanoparticles and their photocatalytic activities. RSC Adv 7:48083–48094
197. Eskandarloo H, Badiei A (2014) Photocatalytic application of titania nanoparticles for degradation of organic pollutants. In: Aliofkhazraei M (ed) Nanotechnology for optics and sensors. One Central Press (OCP), pp 108–132
198. Byrne C, Subramanian G, Pillai SC (2018) Recent advances in photocatalysis for environmental applications. J Environ Chem Eng 6:3531–3555
199. Gaber A, Abdel-Rahim MA, Abdel-Latief M, Abdel-salam MN (2014) Influence of calcination temperature on the structure and porosity of nanocrystalline SnO_2 synthesized by a conventional precipitation method. Int J Electochem Sci 9:81–95
200. Sharma JK, Srivastava P, Ameen S, Akhtar MS, Sengupta SK, Singh G (2017) Phytoconstituents assisted green synthesis of cerium oxide nanoparticles for thermal decomposition and dye remediation. Mater Res Bull 91:98–107

Publisher's Note Springer Nature remains neutral with regard to jurisdictional claims in published maps and institutional affiliations.